JOC The Journal of Organic Chemistry

Evaluation of Substituent Effect in Z-Isomer Stability of Arylazo-1H-3,5-dimethylpyrazoles – Interplay of Steric, Electronic Effects and Hydrogen Bonding

Sudha Devi, Mayank Saraswat, Surbhi Grewal, and Sugumar Venkataramani

J. Org. Chem., **Just Accepted Manuscript** • DOI: 10.1021/acs.joc.7b02604 • Publication Date (Web): 22 Mar 2018

Just Accepted

ACS Publications

is published by the American Chemical Society. 1155 Sixteenth Street N.W., Washington, DC 20036

Evaluation of Substituent Effect in *Z*-Isomer Stability of Arylazo-1*H*-3,5-dimethylpyrazoles – Interplay of Steric, Electronic Effects and Hydrogen Bonding

Sudha Devi†, Mayank Saraswat†, Surbhi Grewal†, and Sugumar Venkataramani*

Department of Chemical Sciences, Indian Institute of Science Education and Research Mohali,

Sector 81, Knowledge City, S.A.S. Nagar, Manauli - 140306, Punjab, India

E-mail: sugumarv@iisermohali.ac.in

Abstract: The electronic and steric effects of aryl substituents, and the influence of hydrogen bonding in *Z*-isomer stability of phenylazopyrazole derivatives have been investigated. In this regard, 38 substituted phenylazopyrazole derivatives and six *N*-methyl phenylazopyrazole (with *meta*-substitutions) have been synthesized. Their photoswitching behavior, photostationary states (PSS) and kinetics of thermal reverse isomerization were evaluated experimentally using UV-Vis and NMR spectroscopic techniques. Furthermore, density functional theory (DFT) computations have been performed for more detailed insights. Despite the presence of substantial substituent effects inferred through Taft and Hammett relationships, concentration dependency in controlling the isomerization rates has also been observed. Kinetics studies at different concentration, solvent effects and computations have confirmed the decisive role of hydrogen bonding and solvent assisted tautomerism in this regard. Through this study, a complex interplay of steric, electronic effects and hydrogen bonding as factors in dictating the stability of *Z*-isomers in arylazo-1*H*-3,5-dimethylpyrazoles has been demonstrated.

Keywords: Phenylazopyrazole, Photoswitching, Isomerization, Substituent effects

Introduction

Light driven processes are very attractive in the development of variety of applications such as molecular machines,[1] data storage,[2] molecular recognition,[3] artificial ion channels,[4] sensors[5] and catalysis[6] etc. Azobenzenes are one of the very important classes of photoswitchable molecules that show light induced reversible switching between *E*- (thermodynamically stable state) and *Z*-isomers.[7] Despite the fact that azobenzenes are well known for more than hundred years,[8] the interest in it is not subsided at all. The main reason is the potential applications of them in key areas such as material chemistry,[9] biochemical applications[10] and medicinal chemistry[11] etc. All such applications completely rely on the photoswitching behavior (forward *E*-*Z*, and the reverse *Z*-*E* isomerization processes) and the thermal stability of *Z*-isomer. Various mechanisms such as rotation, inversion, concerted-inversion, or inversion-assisted rotation with inversion have been proposed for the photochemical isomerization.[12] On the other hand, under thermal conditions, the reverse isomerization happens either through the inversion mechanism, or through rotation mechanism.[13]

The salient features of azobenzene as photoswitchable molecules are robustness in switching, rate of *E*-*Z* forward switching, extent of photostationary state (PSS) and thermal half-life of *Z*-isomer. Based on the gap between π–π* and n–π* transitions of azo group, azoarenes have been classified as azobenzenes (well-separated), aminoazobenzenes (overlapping), and pseudo-stilbenes (nearly degenerate).[14] Such classifications are mainly due to the type of substitutions that can dictate the switching ability as well as the stability of *Z*-isomer. Furthermore, the choice and the introduction of specific substituents such as fluoro and alkoxy at all the four *ortho* positions with respect to azo group can lead to visible light induced

isomerization in azoarenes.[15] Hence, position of the substituent in the aryl ring is equally important in controlling the photoswitching characteristics. For variety of applications, all these properties need to be altered. Replacing arenes with heterocycles is an alternative strategy, which is an emerging area in this regard. Pyridine containing heteroazoarenes are one of the well-known photoswitches that have found many interesting applications.[16] Despite the presence of many literature on the analogous five-membered heteroazoarenes, the studies on them have been limited to synthesis and evaluation of medicinal properties in the past.[17] However, such systems found a considerable attention only after their photoswitching properties have been evaluated. Herges and coworkers have synthesized an imidazole-connected azoarene, which had a long half-life in its *Z*-form.[18] Fuchter and coworkers enhanced the stability of *Z*-isomer upto 1000 days, when they introduced *N*-methyl pyrazole moiety.[19] After these findings, many groups started utilizing them for various light-driven processes and as photoswitches.[20]

Fuchter's group has explored the effects of *N*-methylated five-membered heterocycles towards tuning the photoswitching behavior.[21] Using experimental rate constants and computational data, they investigated the influence of heterocycles on the stability of *Z*-isomer. Recently, König and coworkers have tuned the lifetimes of *Z*-isomer of phenylazoindoles from nanoseconds to days by controlling the hydrazone tautomerization.[13f] Despite the presence of enormous literature on azoarenes and their derivatives, including their mechanistic studies, the general role of substituents in the photoswitching is not explored in a systematic way. Few issues like the choice of substituents in enhancing the *Z*-isomer stability and the role of electronic effects in photoswitching behavior and reverse isomerization can be vital in design and development of azoarene based molecular switches. In order to address these issues,

we have chosen phenylazopyrazole **1d** as our target, which structurally lacks the *N*-methyl group (**1e**) that was previously reported by Fuchter and co-workers.[19] The advantages of this choice are the ease of synthetic access to variety of substituted derivatives, and also the possibility of post-functionalization at pyrazole N-H. Apart from that, the kinetic studies on such NH phenylazopyrazole **1d** showed almost three order of magnitude higher rate constant than that of **1e**, which provide a better opportunity to study the enormous insights into the role of substituents. In this regard, the *modus operandi* of substituents, particularly with respect to the photoswitching behavior, stability of *Z*-isomer, and their influence in the thermal reverse switching of the *Z*-isomer, which are the primary focus of this investigation.

We utilized a common strategy to synthesize various substituted pyrazole based azoarenes in good to excellent yields. The influence of position (*ortho*-, *meta*- and *para*-) and nature (electron donating vs electron withdrawing) of the substituents have been investigated. Also, the role of substituents in photoswitching behavior, thermal reverse isomerization kinetics, and half-lives of the *Z*-isomers has been studied using UV-Vis and NMR spectroscopic techniques. Additionally, computational studies have been carried out in order to get deeper insights and rationalization of these results. Herein, we report the synthesis of wide range of pyrazole based substituted azoarenes, their photoswitching properties and computational studies in understanding the effects of electronic, steric and hydrogen bonding.

Results and Discussion

A. Synthesis:

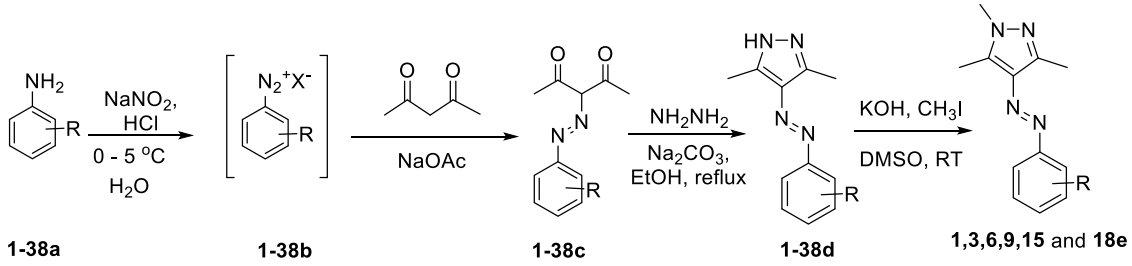

Scheme 1. Synthesis of substituted phenylazopyrazoles **1-38d** and selected *N*-methyl phenylazopyrazoles [R = H(**1e**); 3-F(**3e**); 3-Cl(**6e**); 3-Br(**9e**); 3-OCH_3(**15e**); 3-CF_3(1**8e**)]

A two-step strategy has been adopted to prepare the desired 1*H*-3,5-dimethylpyrazole connected azoarene derivatives. The first and foremost step is to synthesize the arylazoacetylacetone derivatives (**1c-38c**).[22] These derivatives can be accessible through the diazotization of readily available aryl amines, followed by the treatment with acetylacetone (**Scheme 1** and **Table S1** in **SI**). The yields are particularly high when aqueous sodium acetate has been used along with acetylacetone. On reacting the isolated **1c-38c** with hydrazine led to the target pyrazole based substituted heteroazoarene derivatives (**1d-38d**). Additionally, *N*-methylation has been performed at the pyrazole NH using KOH as a base and CH_3I on a set of pyrazole derivatives **1d**, **3d**, **6d**, **9d**, **15d** and **18d**. This led to synthesis of the corresponding *N*-methylated pyrazole connected azoarenes with different *meta*-substitutions **1e**, **3e**, **6e**, **9e**, **15e** and **18e**.

B. Analysis of photoswitching through UV-Vis and NMR spectroscopic techniques:

Traditionally UV-Vis spectroscopic studies play a very important role in understanding the *E-Z* isomerization of azobenzenes. This is because of the

distinguishable spectral features for *E*- and *Z*-isomers, arising due to drastic changes in the electronic structure. In order to understand the effects of substituents on their electronic spectra, the spectral data of the *E*- and *Z*-isomers of phenylazopyrazole derivatives **1-38d** have been compared. For comparison, all the photoswitching and kinetics experiments have been carried out in acetonitrile, and at a temperature of 25 ± 1 ^{o}C in order to minimize the errors due to external parameters. Electronic spectroscopic parameters such as λ_{max} and molar extinction coefficient (ε) have been obtained for all the *E*- and *Z*- isomers in this regard (**Figure 1**, **2**, **Table 1** and **Table S2** in **SI**). Upon irradiation at a wavelength of 365 nm, almost all of the derivatives exhibited *E* to *Z* isomerization. The data on the shifts in the λ_{max} corresponding to π–π* and n–π* absorptions of *Z*-isomers have been included in the table S2 in SI. The ε values of π–π* and n–π* transitions of *Z*-isomers have been estimated based on the PSS composition and its corresponding absorption values.[23] The plots on the absorption maxima vs ε of the individual π–π* transitions of *E*- and *Z*-isomers show that only the former is sensitive to the electronic effects (**Figure 1a** and **1b**). Due to the breaking of conjugation, the azo group in *Z*-isomers is less sensitive to the electronic influence, and so majority of the substituted *Z*-arylazopyrazoles exhibit similar π–π* absorption properties. However, there is a reasonable steric influence, which can be understood from the deviation for those derivatives having *ortho* substituents in the phenyl ring with respect to the parent **1d**. On the other hand, both *E*- and *Z*-isomers show more deviation in the n–π* absorption properties (**Figure 1c** and **1d**) that can be attributed to the electronic effects of substituents on the azo nitrogen.

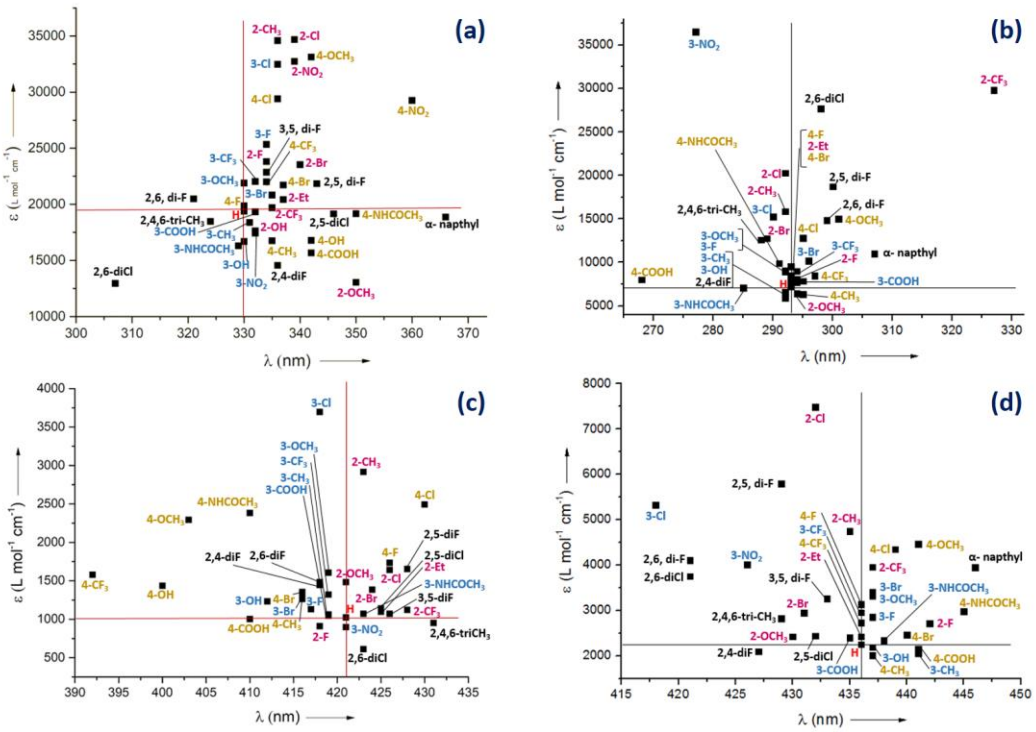

Figure 1. Effect of substituents in the absorption properties of *E*- and *Z*-isomers of the substituted phenylazopyrazoles: (a) and (b) corresponding to π–π* absorptions for *E*- and *Z*-isomers, respectively; (c) and (d) corresponding to n–π* absorptions for *E*- and *Z*-isomers, respectively. (The absorption variation and λ_{max} shifts are separated into four quadrants with respect to the absorbance and λ_{max} of parent **1d** as origin.)

Few derivatives such as 2-hydroxy **11d** and 4-hydroxy phenylazopyrazole **13d** derivatives exhibit minimal spectral changes albeit a small to substantial decrease in their intensities. Interestingly, the spectral features of **11d** with two split-up bands in the π–π* region resemble that of 2-hydroxyazobenzene. The intramolecular hydrogen bonding and/or solvent assisted tautomerization leading to the hydrazone form may be the plausible reason for this behavior.[14] Simillarly 2-nitro **20d** and 4-nitro phenylazopyrazole **22d** also showed a little change in the spectra after irradiation. Presumably, both of them behave like a push-pull type azobenzene, for which the switching rates are expected to be fast. Furthermore, the 3-nitro phenylazopyrazole

21d also showed a very high reverse isomerization (*Z*-*E*) rate. The reasons for this non-switching nature of **20d** and **22d** can be attributed to resonance, whereas inductive effects of the nitro group influence a fast reverse switching in **21d** that renders a push-pull type mechanism. The plausible tautomers and resonance structures governing this behavior of **11d**, **13d**, **20d** and **22d** are indicated. (for details see **SI Scheme S2**)

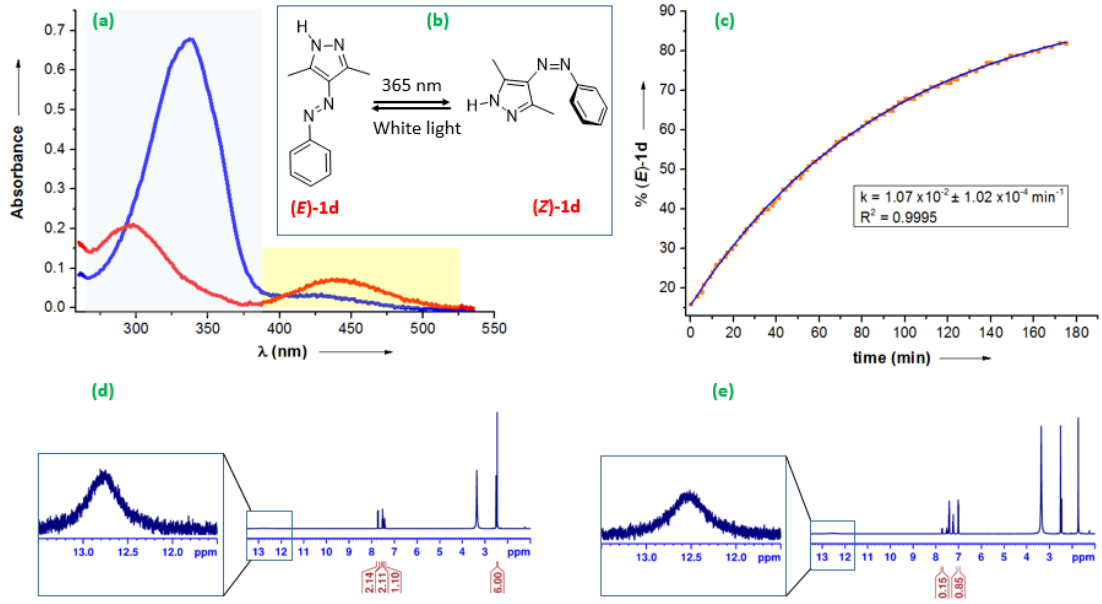

Figure 2. Representative figure on photoswitching in phenylazopyrazole derivative **1d**: (a) Analysis of photoswitching of **1d** in DMSO using UV-Vis spectroscopy (Spectral trace in blue – **(*E*)-1d**; red – after 365 nm irradiation to attain PSS); (b) Reversible photoisomerization of **1d**; (c) First order kinetics trace corresponding to the thermal reverse *Z*-*E* isomerization of **1d** (using NMR spectroscopy); NMR spectrum of **(*E*)-1d** in DMSO-d_6 (d) before irradiation, and (e) after irradiation at 365 nm for 30 minutes.

Table 1. UV-Vis spectroscopic data of *E*- and *Z*-isomers of arylazopyrazole derivatives (**1d-38d**)

S. No.	Compound	R=	*E-isomer*[a]			*Z-isomer*[a]			k^d, min^{-1}	[μM] μmol. L^{-1}
			$\pi-\pi^*$ λ_{max}, (ε)	$n-\pi^*$ λ_{max}, (ε)	*E-Z* PSS[b] (%*Z*)	$\pi-\pi^*$ λ_{max}	$n-\pi^*$ λ_{max}	*Z-E* PSS[c] (%*E*)		
1	**1d**	H	330 (19369 ± 278)	421 (1199 ± 57)	85	293	436	77	$1.31 \times 10^{-3} \pm 5.99 \times 10^{-6}$	37
2	**2d**	2-F	334 (23807 ± 862)	418 (910 ± 108)	90	287	442	75	$2.73 \times 10^{-3} \pm 9.48 \times 10^{-6}$	29
3	**3d**	3-F	334 (25338 ± 2314)	417 (1129 ± 116)	87	292	437	74	$1.85 \times 10^{-3} \pm 2.35 \times 10^{-5}$	29
4	**4d**	4-F	330 (19853 ± 278)	426 (1532 ± 26)	85	293	436	96	$1.62 \times 10^{-3} \pm 1.24 \times 10^{-5}$	27
5	**5d**	2-Cl	339 (34674 ± 681)	426 (1641 ± 125)	84	292	432	86	$4.03 \times 10^{-3} \pm 1.58 \times 10^{-5}$	21
6	**6d**	3-Cl	336 (32797 ± 278)	418 (3694 ± 185)	80	290	418	77	$1.14 \times 10^{-2} \pm 7.89 \times 10^{-5}$	19
7	**7d**	4-Cl	336 (29398 ± 1823)	430 (2397 ± 106)	90	295	439	94	$1.67 \times 10^{-3} \pm 3.04 \times 10^{-5}$	23
8	**8d**	2-Br	340 (23530 ± 1509)	424 (1383 ± 83)	88	289	431	72	$4.29 \times 10^{-3} \pm 1.13 \times 10^{-5}$	22
9	**9d**	3-Br	335 (20818 ± 1147)	416 (1293 ± 34)	86	296	437	73	$5.87 \times 10^{-2} \pm 4.82 \times 10^{-4}$	24
10	**10d**	4-Br	337 (21721 ± 1530)	416 (1355 ± 52)	92	293	440	72	$1.79 \times 10^{-3} \pm 5.39 \times 10^{-6}$	31
11	**11d**	2-OH**	332 (17638) 366 (16042)	-	-	-	-		-	39
12	**12d**	3-OH	330 (16678 ± 1556)	412 (1179 ± 52)	86	292	437	69	$2.88 \times 10^{-3} \pm 1.96 \times 10^{-5}$	38
13	**13d**	4-OH***	342 (16786)	400 (1433)	-	-	-		-	39
14	**14d**	2-CF_3	335 (19703 ± 1221)	428 (1122 ± 26)	41	327	437	87	$3.28 \times 10^{-1} \pm 7.12 \times 10^{-3}$	31
15	**15d**	3-CF_3	332 (22045 ± 392)	419 (1320 ± 84)	83	294	436	86	$2.65 \times 10^{-3} \pm 9.46 \times 10^{-6}$	24
16	**16d**	4-CF_3	334 (22010 ± 858)	392 (1578 ± 53)	79	297	436	80	$2.96 \times 10^{-2} \pm 1.15 \times 10^{-4}$	29
17	**17d**	2-OMe	350 (13044 ± 338)	421 (1483 ± 42)	92	294	430	56	$1.04 \times 10^{-3} \pm 1.72 \times 10^{-5}$	45
18	**18d**	3-OMe	330 (21893 ± 364)	419 (1605 ± 3)	85	292	437	65	$2.97 \times 10^{-3} \pm 2.00 \times 10^{-5}$	24
19	**19d**	4-OMe	342 (33110 ± 1817)	403 (2293 ± 68)	92	301	441	68	$1.20 \times 10^{-3} \pm 1.22 \times 10^{-5}$	16
20	**20d**	2-NO_2***	339 (32724)	-		-	-	-	-	41
21	**21d**	3-NO_2**, [e]	332 (17420 ± 630)	421 (897)	24	-	426	91	$1.04 \times 10^{-3} \pm 1.72 \times 10^{-5}$	37
22	**22d**	4-NO_2***	360 (29247)	-		-	-	-	-	33
23	**23d**	2-CH_3	336 (34578 ± 3434)	423 (2914 ± 197)	92	292	435	80	$6.92 \times 10^{-3} \pm 1.16 \times 10^{-5}$	18
24	**24d**	3-CH_3	331 (18375 ± 1608)	419 (1046 ± 35)	88	292	441	61	$1.99 \times 10^{-3} \pm 1.15 \times 10^{-5}$	30
25	**25d**	4-CH_3	335 (16747 ± 2099)	416 (1262 ± 18)	90	295	437	73	$1.45 \times 10^{-3} \pm 3.24 \times 10^{-6}$	31
26	**26d**	3-CO_2H	332 (19329 ± 235)	419 (1045 ± 15)	81	295	435	65	$3.04 \times 10^{-2} \pm 6.50 \times 10^{-5}$	27
27	**27d**	4-CO_2H	342 (15675 ± 967)	410 (1002 ± 66)	83	300	441	81	$4.41 \times 10^{-2} \pm 1.22 \times 10^{-4}$	38
28	**28d**	3-NHAc	329 (16296 ± 858)	423 (1024 ± 72)	86	285	438	78	$5.44 \times 10^{-2} \pm 1.43 \times 10^{-4}$	34
29	**29d**	4-NHAc	350 (19166 ± 886)	410 (2382 ± 46)	91	303	445	68	$1.44 \times 10^{-3} \pm 4.99 \times 10^{-6}$	36
30	**30d**	2-Et	337 (20424 ± 1608)	425 (1096 ± 57)	92	293	436	74	$1.30 \times 10^{-2} \pm 1.08 \times 10^{-5}$	29
31	**31d**	2,4,6-triMe	324 (18479 ± 881)	431 (950 ± 125)	79	288	429	77	$3.62 \times 10^{-3} \pm 5.46 \times 10^{-6}$	26
32	**32d**	Ar = α-Np	366 (18852 ± 882)	-	89	307	446	72	$4.35 \times 10^{-3} \pm 3.69 \times 10^{-6}$	32
33	**33d**	2,5-diCl	346 (19153 ± 419)	425 (1140 ± 43)	92	294	432	68	$4.45 \times 10^{-2} \pm 3.23 \times 10^{-5}$	30
34	**34d**	2,6-diCl	307 (12943 ± 732)	423 (609 ± 38)	33	298	421	92	$1.89 \times 10^{-3} \pm 2.52 \times 10^{-5}$	44
35	**35d**	2,4-diF	336 (14567 ± 635)	418 (1442 ± 34)	85	292	427	69	$3.26 \times 10^{-3} \pm 9.69 \times 10^{-6}$	36
36	**36d**	2,5-diF	343 (21844 ± 1048)	428 (1653 ± 35)	66	300	429	77	$2.83 \times 10^{-1} \pm 2.31 \times 10^{-3}$	26
37	**37d**	2,6-diF	321 (20491 ± 559)	418 (1482 ± 37)	62	299	421	81	$6.46 \times 10^{-3} \pm 1.21 \times 10^{-5}$	26
38	**38d**	3,5-diF	334 (22857 ± 1168)	426 (1069 ± 63)	56	294	433	84	$8.27 \times 10^{-2} \pm 3.77 \times 10^{-4}$	23

[a]The values of λ_{max} are given in nm and ε in $L.mol^{-1}.cm^{-1}$; [b]PSS for *E*-*Z* isomerization has been estimated at 365 nm[23]; [c]PSS for *Z*-*E* isomerization has been estimated at white light (CFL lamp) irradiation with 2-5% uncertainty[23]; [d]Rate constant in CH_3CN at 25 ± 1 °C; [e]Kinetics has been measured in DMSO at 23 ± 1 °C. (Ar = α-Np is α-naphthyl; (**Upon 365 nm irradiation, the absorptions showed a decrease with the appearance of isosbestic points; ***For 4-OH derivative, photoirradiation did not lead to any spectral change)

The photoswitching studies have also been carried out using NMR spectroscopy.[24] Both photoswitching and reverse thermal isomerization kinetics have been studied in CD_3CN at 25 °C. In order to understand the influence of the substituents in the structural features of the *E*- and *Z*-isomers, a closer inspection at the NMR spectral analysis was carried out. Upon switching from *E*- to *Z*-isomer, the *ortho*-protons of the aryl group, the two-methyl groups of the pyrazoles and also the N-H protons exhibited major shifts towards shielding regions. In spite of showing shifts upon isomerization from *E* to *Z*, the *meta*- and *para*-protons of the aryl group are not considered in this analysis due to overlapping nature of the signals. The changes in the chemical shift values (Δδ) for all the substituents that we studied are included (**Table 2**). The results showed that the *ortho* proton showed a larger upfield shift when electron-withdrawing substituent is present either at *ortho* or *meta* position. Also, the same effect is observed, when electron-donating power increases for the substituent at the *para* position. Upon isomerization, the two-methyl groups showed upfield shifts in the range between 0.67 and 0.72, except for 3,5-difluoro substituted system that showed a shift of 0.62. This clearly indicates that the methyl groups of the pyrazoles showed less perturbation upon isomerization due to the remote distance from the position of substituents at the aryl ring. Also, their shifts further confirm that

the role of steric factor, which is nearly equal in all the cases irrespective of the position of the substituents. Similarly, N-H protons also showed only a negligible effect in the chemical shift values upon varying the substituents. The same trend was observed in the case of *N*-methylated derivatives as well. For all these molecules, *Z*-*E* reverse isomerization kinetics have been followed and the rates have been tabulated (**Table S6** in **SI**). However, we found that the rates are quite different from the UV-Vis kinetics experiments, which can be attributed to electronic and steric effects apart from the difference in the concentration and the reasons are explained in the section-D and E.

Table 2. NMR spectroscopic data of the selected protons of *E*- and *Z*-isomers of different substituted phenylazopyrazoles and *N*-methyl phenylazopyrazoles

S. No.	Compound	Substituent	Conversion[a]	N – H region[b]			CH_3 region[b]			Aromatic region[b] (*ortho*–H)		
				(*E*)-	(*Z*)-	Δδ	(*E*)-	(*Z*)-	Δδ	(*E*)-	(*Z*)-	Δδ
1	**1d**	H	89	10.83	10.66	0.17	2.49	1.77	0.72	7.77	7.00	0.77
2	**2d**	2-F	85	10.88	10.71	0.17	2.49	1.81	0.68	7.72	6.94	0.78
3	**5d**	2-Cl	81	10.88	10.72	0.16	2.51	1.83	0.68	7.69	6.66	1.03
4	**14d**	2-CF_3	69	10.93	10.85	0.08	2.49	1.79	0.70	7.83	6.70	1.13
5	**3d**	3-F	85	10.88	10.69	0.19	2.49	1.81	0.68	7.63	6.84	0.79
6	**6d**	3-Cl	89	10.88	10.70	0.18	2.49	1..81	0.68	7.72	6.95	0.77
7	**9d**	3-Br	77	10.89	10.73	0.16	2.49	1.81	0.68	7.76	6.99	0.77
8	**15d**	3-CF_3	92	10.90	10.71	0.19	2.50	1.78	0.72	8.02	7.21	0.81
9	**18d**	3-OCH_3	63	10.76	10.63	0.13	2.49 **3.85**[c]	1.81 **3.72**[c]	0.68 **0.13**[c]	7.38 **7.39**[d]	6.59 **6.55**[d]	0.79 **0.84**[d]
10	**4d**	4-F	85	10.83	10.65	0.18	2.48	1.80	0.68	7.81	7.08	0.73
11	**7d**	4-Cl	86	10.85	10.67	0.18	2.48	1.80	0.68	7.76	7.02	0.74
12	**10d**	4-Br	86	10.83	10.67	0.16	2.48	1.80	0.68	7.67	6.95	0.72
13	**16d**	4-CF_3	88	10.92	10.72	0.20	2.50	1.79	0.71	7.91	7.17	0.74
14	**19d**	4-OCH_3	62	10.71	10.59	0.12	2.47 **3.85**[c]	1.80 **3.78**[c]	0.67 **0.07**[c]	7.76	6.89	0.87
15	**36d**	2,5-diF	89	10.94	10.77	0.17	2.49	1.80	0.69	7.47	6.82	0.65
16	**38d**	3,5-diF	80	10.94	10.78	0.16	**2.48**	**1.86**	**0.62**	7.40	6.67	0.73

				N – H region[b]			CH_3 region[b]			Aromatic region[b] (*ortho*–H)		
17	**1e**	H	26	3.73	3.60	0.13	2.41 2.55	1.47 2.15	0.94 0.40	7.76	7.02	0.74
18	**3e**	3-F	35	3.73	3.61	0.12	2.41 2.55	1.50 2.10	0.91 0.40	7.63	6.86	0.77
19	**6e**	3-Cl	45	3.73	3.62	0.11	2.40 2.55	1.49 2.11	0.91 0.44	7.72	6.96	0.76
20	**9e**	3-Br	51	3.73	3.62	0.11	2.40 2.55	1.49 2.11	0.91 0.44	7.76	6.99	0.77
21	**15e**	3-CF_3	62	3.74	3.61	0.13	2.42	1.46	0.96	8.05	7.41	0.64

22	**18e**	3-OCH_3	76	3.73	3.60	0.13	2.57 2.41 2.55	2.08 1.51 2.08	0.47 0.90 0.47	7.38	6.60	0.78

[a]*E-Z* conversion during photoisomerization using 365 nm at PSS; [b]Chemical shift values are in ppm; [c]Bold = OMe protons; [d]Two distinct *ortho* protons have been observed (All the spectra have been recorded in CD_3CN at 298 K in 400 MHz NMR).

C. Computational Studies:

In order to understand the effects of the substituents in spectral properties, photoswitching behavior and also the structural aspects, DFT calculations have been performed. Attention was paid to those substituents, for which both NMR and UV-Vis photoswitching studies have been performed. In this regard, we have optimized the structures of both *E*- and *Z*-isomers of the phenylazopyrazole derivatives to the minima. The energy relationship between the HOMO, LUMO and HOMO-1, have been tabulated for various substitutions (**Table S4** in **SI**). The closer inspection at the MOs of the *E*-isomer revealed that the HOMO, LUMO and HOMO-1 can be attributed to π–, π*– and n–orbitals, respectively (**Figure 3a**). On the other hand, the *Z*-isomer showed a change in the order, where the HOMO and LUMO can be attributed to n– and π*-orbital, respectively. However, the HOMO-1 showed a mixed character of n– and π–orbitals. In the case of *E*-isomers, the energy gaps corresponding to π–π* (HOMO – LUMO gap) and n–π* (HOMO-1 – LUMO gap) are found to be nearly unperturbed upon *meta*-substitution, whereas, the *para*-substitutions led to a reasonable effect in the energy gap. This is in line with our experimentally observed spread of λ_{max} corresponding to π–π* and n–π* transitions, for which the *meta*-substitution led to a smaller changes, whereas the *para*-substitutions caused larger deviations in the shifts.

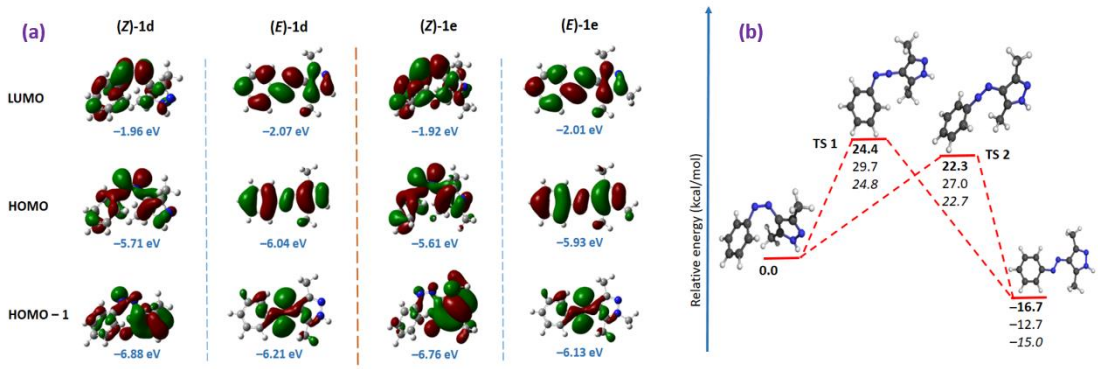

Figure 3. (a) Molecular orbitals corresponding to HOMO, LUMO and HOMO-1 of *E*- and *Z*- isomers of **1d** and **1e**. The orbital energies (in eV) are indicated. (All the orbitals and their corresponding energies are obtained at B3LYP/6-311G(d,p) level of theory) (b) Computed inversion barrier for the thermal reverse isomerization of **1d** (The relative energies with respect to *Z*-isomer are given; Bold – B3LYP/6-311G(d,p); Normal – M06-2X/6-311G(d,p); Italics – B3LYP/6-311G(d,p) in CH_3CN, solvent model)

In the case of *Z*-isomers, computationally estimated energy gaps (HOMO – LUMO gap and HOMO-1 – LUMO gap) showed more deviations for *para* substitutions. This is once again reflected in the observed changes in the UV-Vis absorption maxima of both π–π* and n–π* transitions in the case of *para*-substituted derivatives. However, except OCH_3 group, rest of the substituents at *meta*- position exhibited no deviation with respect to computational and the experimental observations in this regard. The corresponding *N*-methyl phenylazopyrazoles with *meta*- substitutions also showed less perturbation with respect to the energy gaps of the orbitals.

Since the thermal reverse isomerization is depending on the geometries of the *Z*-isomer, we tried to understand the molecular properties of them that can influence the stability of *Z*-isomer and also the kinetics.[21] In this regard,

various parameters such as dihedral angles, charges at the azo nitrogen and bond orders have been compared for *meta* and *para* substituted *Z*-isomers (**Table S3** in **SI**). Indeed, attempts have been made to relate those individual properties with the rate constants; however, in none of the cases we observed a good correlation.

Apart from the structural insights through computations, we have estimated the thermal barriers and rate constants for the conversion of *Z*- to *E*-isomer through inversion mechanism at the azo nitrogen.[25] Since all the derivatives utilized in this investigation are unsymmetrical azoarenes, there are two possible inversion barriers. Among them, the inversion happens at the azo nitrogen connected to the aryl group is found to be the minima in majority of the cases (**Figure 3b** and **Table S9** in **SI**). The only exception was observed in the case of 4-OCH_3 substituted system, where the inversion at pyrazole ring connected azo nitrogen was found to be the lower energy pathway. In all the cases, the transition state was found to acquire a twisted geometry, due to the presence of two methyl groups in the pyrazole. We considered both the transition states and obtained weighted average barriers for estimating the rate constants.[26]

D. Effects of substituents and hydrogen bonding in the stability of *Z*-isomers:

The effects of substituents on the stability of *Z*-isomer have been studied through thermal reverse isomerization kinetics using UV-Vis spectroscopy in CH_3CN at 25 ± 1 ^oC. All the substituted phenylazopyrazole derivatives have been switched from *E*- to *Z*-isomer using a light of wavelength 365 nm, followed by the thermal reverse isomerization kinetics have been measured. The

photoisomerization has been performed in such a way that maximum *Z*-isomer conversion is observed or the irradiation is done until the establishment of photostationary state (PSS). Upon the thermal reverse isomerization, the exponential rate of formation of the *E*-isomer has been plotted at an absorbance λ_{max} corresponding to the $\pi-\pi^*$ transition of the *E*-isomer. Using the first order rate constant, the half-life of the *Z*-isomer has also been deduced. For comparison, the kinetics experiments have been studied for the selected substituents using NMR spectroscopy and also computations (**Table S6** in **SI**). For minimizing the solvent effects, the kinetics experiments have been done in CD_3CN (for NMR) experiments and using acetonitrile as solvent model (for computations). In the case of NMR studies, a CD_3CN solution of *E*-isomer in a quartz NMR tube has been irradiated at 365 nm to reach a PSS, subsequently the formation of *E*-isomer has been followed. Using the integral ratios of identical protons of both the isomers (often aromatic *ortho* protons, which are non-overlapping), the growth rate of *E*-isomer has been estimated (**Figure S3** of supporting information).

For understanding the effects and influence of the substituents in the stability of *Z*-isomer, a quantitative relationship of the involvement of steric and electronic effects comprising resonance, field and inductive effects, respectively in the reverse isomerization kinetics is necessary. In this regard, we have considered the Taft[27] (for *ortho* substitution) and Hammett[28] (for *meta* and *para* substitutions) relationships. For the *ortho* substituted derivatives, a Taft plot has been plotted between the $\log(k_R/k_{Me})$ vs the steric substituent constant (E_s), where k_R is the isomerization rate of the *ortho* substituted phenylazopyrazole derivatives and k_{Me} is the rate corresponding to the 2-CH_3 derivative **23d**

(**Figure 4**). The resulting plot showed a good correlation with a negative slope indicating the influence of steric factors (arising from the *ortho* substitutions at the phenyl ring) in the thermal reverse isomerization processes. This indicates that the transition state possesses less steric repulsion relative to the corresponding *Z*-isomer. Indeed, these results are in consistent with the earlier reports on azoheteroarenes possessing *ortho* substituents, whose rates of thermal isomerization were high.[21] Due to this reason, for the NMR and computational kinetics studies, we have considered only the electronic effects and so focused on the *meta* and *para* substituents.

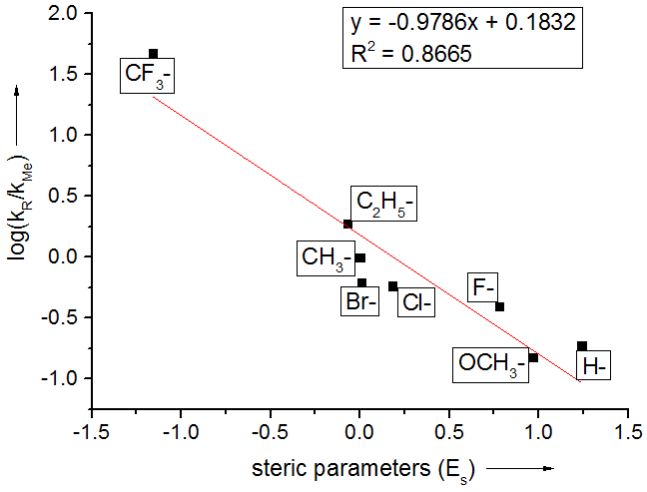

Figure 4. Taft plot for the steric effects in the kinetics of reverse thermal isomerization of phenylazopyrazole **1d** and their *ortho*-substituted derivatives using UV-Vis spectroscopy in CH_3CN at 25 ± 1 °C.

For *meta* and *para* substituents, we have considered the Hammett relationship by plotting $\log(k_R/k_H)$ vs substituent constants. When the kinetics rate constants from UV-Vis spectroscopic data have been utilized, we observed a non-linear correlation, however, it showed a reasonable positive trend in both the cases (**Figure S6** in **SI**). Based on the linear free energy relationships, it is very clear that electronic factors strongly influence the reaction rates. Either

change in the mechanism (rotation vs inversion) upon changing the substituents or the combined perturbations due to solvents (solvent assisted tautomerism) and steric factors (due to the two methyl groups) along with the electronic effects could be the reason for the non-linearity.[29] To understand this behavior, we have plotted the Hammett relationship using computed rate constants (**Figure 5d** and **5e**). Not only those plots showed a very good correlation with positive slopes for both *meta*- and *para*- substituted arylazopyrazoles, but also confirmed the presence of substantial electronic effects in the rate of isomerization. Apparently, accumulation of negative charges has been observed at the two azo nitrogens for both the transition states (**Table S5** in **SI**).

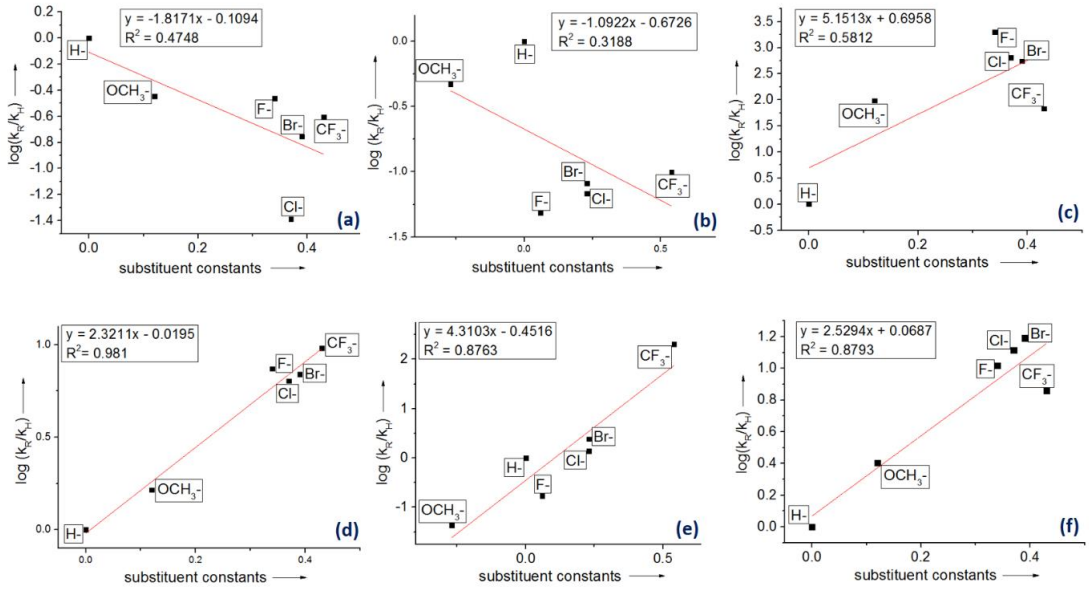

Figure 5. Substituent effects in kinetics of reverse thermal isomerization of phenylazopyrazole and *N*-methyl phenylazopyrazole derivatives using NMR spectroscopy in CD_3CN at 298 K: Hammett plots for (a) *meta* substitutions; (b) *para* substitutions; (c) *N*-methylated *meta* substitutions; using computations at B3LYP/6-311G(d,p) level of theory: Hammett plot for (d) *meta* substitutions; (e) *para* substitutions; (f) *N*-methylated *meta* substitutions.

On contrast, the Hammett relationships for *meta* and *para* substituted phenylazopyrazoles using rate constants derived from NMR revealed a trend with a negative slope (**Figure 5a** and **5b**). This trend is completely opposite to the computational (in gas phase) and UV-Vis (in acetonitrile) based relationships. The major difference between the rate of the reverse isomerization kinetics in NMR and UV-Vis spectroscopic experiments can be the concentration. For UV-Vis spectroscopy, the experiments have been performed at μM concentration, whereas, for NMR studies, we have utilized a concentration range of mM. The higher concentration, in principle can influences the rates in the following ways namely, supramolecular interactions through π-stacking or through hydrogen bonding. Due to the presence of two methyl groups, the π-stacking interactions can be unfavourable. However, the presence of a free N-H in phenylazoprazole derivatives can potentially form hydrogen bonding at various sites that include azo nitrogens, pyrazole nitrogen and the hydrogen bond acceptor substituents, if any. Also, due to the steric reasons only the azo nitrogens of *Z*-isomer can accept intermolecular hydrogen bonding. This assumption is particularly fitting very well with the change in the slope for Hammett plots, upon increasing the concentration. Under such circumstances, the charge at the inverting azo nitrogen center is expected to gain more positive values or less negative charge, which is in perfect corroboration with the computed charges at azo nitrogen centers. The hydrogen bonding at one of the azo nitrogen's led to lowering of negative charges at the adjacent nitrogen atom, which undergoes inversion (**Table S5** in **SI**). Apart from the substantial

electronic effects, the hydrogen bonding is expected to play a crucial role in the reverse switching of phenylazopyrazole derivatives.

In order to downplay the hydrogen bonding, six *meta* substituted *N*-methyl phenylazopyrazole derivatives (**1e**, **3e**, **6e**, **9e**, **15e** and **18e)** have been chosen and Hammett relationship has been studied. Since the unsubstituted *N*-methyl derivative **1e**, has been extensively studied by Fuchter and coworkers, the rate constant for its thermal isomerization has been taken from their studies.[19, 21] For the rest of the derivatives, the *Z-E* isomerization kinetics have been performed in CD_3CN at 298 K and the Hammett relationship has been plotted (**Figure 5c**). The results for *N*-methylated derivatives revealed that the plot once again reverted back to a positive slope, which is similar to their corresponding computational plot in figure 5f. This clearly demonstrates the role of pyrazole NH in hydrogen bonding.

E. Concentration dependency and solvent effects in *Z*-isomer stability:

During our investigations on photoswitching and reverse isomerization behavior of substituted phenylazopyrazoles, we realized the importance of effects of concentration. Apart from the reverse isomerization rate, photoswitching efficiency also strongly depend on the concentration. In this regard, we did the concentration dependent kinetics for the compound **1d** (**Figure S7** in **SI**). The results suggested that the half-life of the **(*Z*)-1d** decreases by three times (21.6 min to 8.2 min) when the concentration increases by approximately 14 times (0.004 M to 0.055 M). The results clearly confirm that at the higher concentration, the *Z-E* isomerization rate constant increases and the half-life of *Z*-isomer decreases. Besides, we observed a marginal downfield shift in the N-H proton of **1d**, whereas other protons showed no significant shifts upon increasing the concentration. These observations clearly further confirms

the possibility of hydrogen bonding involving pyrazole N-H. To understand the mode of hydrogen bonding in concentration dependency, we estimated the association constant of the hydrogen bonding dimer of the **(*E*)-1d**. Using NMR spectroscopy, the spectral shifts of the pyrazole NH protons accompanying the concentration changes (relative to the residual protons of the solvent) have been considered. Using the open access web based bindfit program, a non-linear fitting process has been executed in this regard.[30] The resulting binding constant for the 1:1 **(*E*)-1d** dimer was found to be $1.47 \times 10^{-3} \pm 1.69 \times 10^{-4}$ L mol^{-1}. (See the details in **Figure S9** and **S10** in **SI**). In order to differentiate the solute-solute and solute-solvent interactions, the phenylazopyrazole **1d** has been subjected to NMR kinetics in DMSO-d_6, which is known for the breaking of intermolecular hydrogen bonding (**Figure 1**). As a result, the half-life of the *Z*-isomer has increased and the rate of reverse isomerization has been decreased.

To emulate such hydrogen bonding possibilities and also to understand the effects of it in the thermal reverse isomerization, computations are highly desired. In this regard, we explored the barriers for the thermal isomerization step using simple pyrazole as a model compound, with and without hydrogen bonding (**Figure 6**). From those calculations, we inferred that the thermal isomerization barriers indeed showed a lowering of Gibbs free energy of activation upon hydrogen bonding. Although the changes in the barrier energies are found to be very small, it indeed significantly influenced the rate constants and half-lives. Similar trend has also been observed when actual dimeric phenylazopyrazole dimers are invoked in the computations (See **Figure S4** in **SI)**

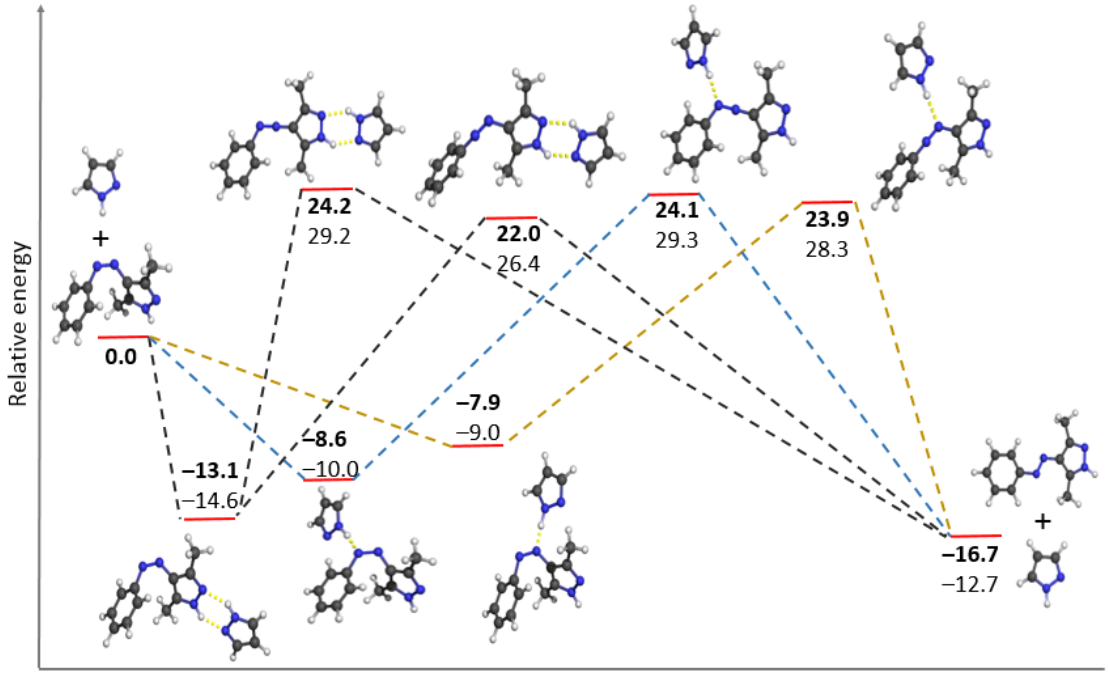

Figure 6. Effects of hydrogen bonding in the *Z-E* thermal isomerization in phenylazopyrazoles: Computed barriers for the thermal reverse isomerization with the H-bonding of pyrazole at various positions in phenylazopyrazole (The TS barriers (in kcal/mol) for various channels are indicated with respect to ***E*-1d** + pyrazole (individual hydrogen bonded complexes); Bold – B3LYP/6-311G(d,p); Normal – M06-2X/6-311G(d,p)

In the same context, we have also studied the effects of solvents in the thermal reverse *Z-E* isomerization rate by varying the polarity of the solvents at the identical concentration. The results are tabulated (**Table 3** and **Figure S11** in **SI**). Based on the results, the polar protic solvents such as ethanol and methanol showed a maximum influence such that **1d** underwent fast thermal *Z-E* isomerization. Indeed in methanol the rate could not be determined. On the other hand, rate constants are estimated to be smaller in the case of non-polar solvents such as toluene, whereas the polar aprotic solvents still influence the rate from moderate to high.

Table 3. Solvent effects in the UV-Vis spectroscopic thermal reverse isomerization (*Z*-*E*) rates of phenylazopyrazole **1d** and N-methyl phenylazopyrazole **1e**

S. No.	Solvent[a]	Solvent Parameters[b]				k^a (min^{-1})	k^c (min^{-1})
		α	β	π*	E_T^N		
1.	Acetonitrile	0.19	0.40	0.66	0.460	$7.27 \times 10^{-3} \pm 2.50 \times 10^{-5}$	-
2.	Chloroform	0.20	0.10	0.69	0.259	$2.67 \times 10^{-3} \pm 1.26 \times 10^{-5}$	-
3.	Dichloromethane	0.13	0.10	0.73	0.309	$2.20 \times 10^{-3} \pm 1.18 \times 10^{-5}$	-
4.	DMF	0.00	0.69	0.88	0.386	$6.72 \times 10^{-2} \pm 1.20 \times 10^{-3}$	$4.29 \times 10^{-3} \pm 6.83 \times 10^{-5}$
5.	Ethyl acetate	0.00	0.45	0.45	0.228	$1.00 \times 10^{-2} \pm 1.35 \times 10^{-5}$	-
6.	Ethanol	0.86	0.75	0.54	0.654	$8.37 \times 10^{-2} \pm 2.55 \times 10^{-5}$	$2.32 \times 10^{-3} \pm 1.77 \times 10^{-4}$
7.	Methanol	0.98	0.66	0.60	0.762	–	
8.	Toluene	0.00	0.11	0.49	0.099	$3.00 \times 10^{-3} \pm 1.31 \times 10^{-5}$	$5.42 \times 10^{-3} \pm 1.16 \times 10^{-4}$
9.	THF	0.00	0.55	0.55	0.207	$1.20 \times 10^{-3} \pm 1.84 \times 10^{-5}$	-
10.	DMSO	0.00	0.76	1.00	0.444	$9.73 \times 10^{-3} \pm 4.21 \times 10^{-4}$	$4.12 \times 10^{-3} \pm 1.10 \times 10^{-4}$

[a]All the solutions of **1d** have been studied in different solvents at an identical concentration (29 μM) and the rates have been measured at 25 ± 1 °C; [b]Solvent parameters are the Kamlet–Taft parameters for hydrogen bonding ability (α) and hydrogen donating ability (β) and the solvatochromism scales π* and E_T^N; [c]All the solutions of **1e** have been studied in different solvents at an identical concentration (34 μM) and the rates have been measured at 60 ± 1 °C.

To relate the effects of solvents in the reverse isomerization,[31] various properties of the solvents such as Kamlet–Taft parameters for hydrogen bonding ability (α) and hydrogen donating ability (β) and the solvatochromism scales π*[32-34] and E_T^N[35] have been considered. Previous studies on limited number of azobenzenes revealed that the solvent polarity rather than the viscosity of the solvents is vital for the thermal isomerization kinetics.[31b,c] The correlation between the individual parameters with the

rate constants, (plots of lnk vs solvent parameters) have been clearly showed a remarkable influence of hydrogen bonding effects (**Figure 7** and **Figure S12** in **SI**). Particularly the solvents with higher proton donating abilities strongly influence the reverse isomerization rates. The exceptions in the case of DMSO and THF can be rationalized on the basis of their hydrogen bond breaking abilities. All these observations are in consistent with the results related to the aryazoimidazoles[36] and phenylazoindoles[13f], where the involvement of protic molecules has been proposed for fast isomerization through tautomerization mechanism.

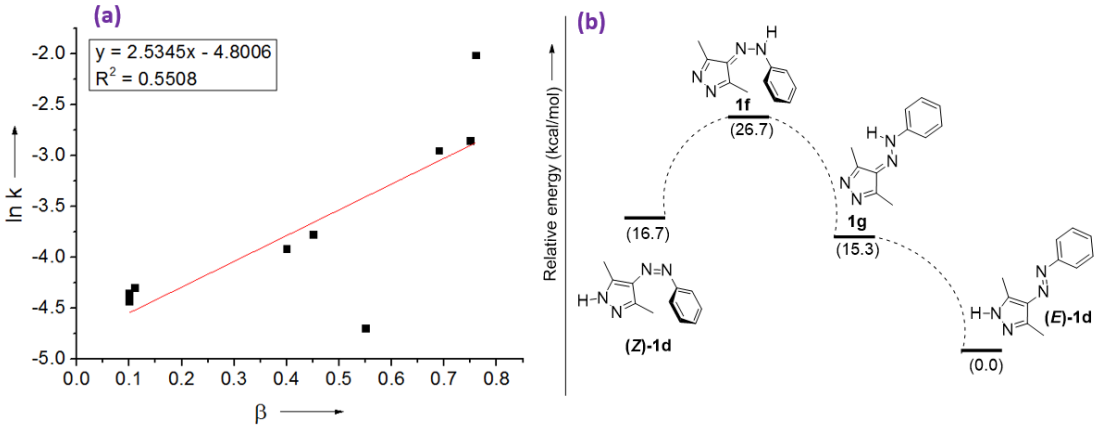

Figure 7. Solvent effects in the thermal *Z*-*E* isomerization rate of **1d**. (a) Graphical plots showing the relation between lnk and the Kamlet–Taft parameters for hydrogen donating ability, β; (b) Possible mechanism for the solvent assisted thermal *Z*-*E* isomerization through tautomerization (Relative energies in kcal/mol are computed at B3LYP/6-311G(d,p) level of theory)

In a similar way, solvent effects have been studied for the *N*-methylated derivative **1e**. Due to the very slow rate of *Z*-*E* isomerization, the studies have been performed at 60 ^{o}C (**Figure S11** in **SI**). Hence, the experiments have been performed only in low volatile solvents such as DMSO, DMF, toluene and ethanol. Remarkably, the isomerization rates in all these solvents have been estimated to be in the same order (**Table 3**). All these data clearly demonstrate that the hydrogen bonding and

proton donation are the most influential factors for the faster *Z*-*E* isomerization kinetics. Particularly when the azo groups are forming hydrogen bonding, the rates are very high, whereas, the non-covalent interactions involving the solvents and the pyrazole-NH decrease the thermal isomerization rates.

Based on all these studies, we obtained the following general trends: (1) Hydrogen bonding either increases the rate of reverse isomerization and/or inhibits the photoswitching efficiency; (2) Any solvent that can protonate azo nitrogen or forming hydrogen bonding with them increases the rate of the thermal reverse isomerization through tautomerization mechanism; (3) At higher concentration, the hydrogen bonding interactions competitively play important roles in deciding the photoswitching behavior. For designing new photoswitches, the intermolecular hydrogen bonding possibilities may also need to be taken care, in particular, for controlling the *Z*-isomer stability.

Conclusions:

In summary, we have synthesized 38 substituted phenylazopyrazole derivatives and six *N*-methylated phenylazopyrazole derivatives using a two/three-step synthetic method with good to excellent yields. The UV-Vis spectroscopic investigations on those molecules revealed the importance of steric factor in attaining highly strained *Z*-isomer geometries that favor a faster reverse switching. Taft plot clearly proved the release of steric factor during reverse isomerization in *ortho* substituted phenylazopyrazoles. On contrast, the *meta* and *para* substituted azopyrazoles undergo reverse isomerization with electronic influence, however, Hammett plot exhibited a deviation from linear correlation. Substantial influences of electronic effects have been further confirmed by Hammett plots using computed rate constants for the selected *meta* and *para*-substituted derivatives. The NMR

spectroscopic studies also revealed the influence of electronic effects in thermal reverse isomerization, however, the slopes are completely opposite to that of UV-Vis spectroscopic and computational studies. The similar studies on the *N*-methylated derivatives with *meta* substitution reverted back to the positive slope in the Hammett plot. Concentration dependency in half-life of the *Z*-isomer, NMR shifts in the pyrazole NH, solvent effects and also the computations clearly demonstrate the decisive role of hydrogen bonding. The solvent or any proton donor can influence the isomerization rate through assisting in the protonation leading to tautomerization. Thus, the non-linear behavior in the substituent effects of isomerization rate and *Z*-isomer stability can be due to a combined effect of steric, electronic effects and the hydrogen bonding. At higher concentrations, hydrogen bonding dominates and at lower concentrations, apart from the electronic and steric factors, solvent assisted tautomerization also prevail in deciding the rate of thermal reverse isomerization, in turn, the stability of *Z*-isomers.

Computational Methods:

All the structures (reactants, products and transition states) optimization have been performed at density functional theory[37] with B3LYP[38], M06-2X[39] functional with 6-311G(d,p)[40] basis set in gas phase as well as in solvent phase[41]. All the geometry optimization have been verified to minima/transition state by frequency calculations. The transition states[42] have also been verified by computing the intrinsic reaction coordinates (IRC).[43] Natural bond orbital (NBO)[44] calculations were performed at same level of theory in order to obtain the Wiberg index[45] for selected azopyrazole derivatives. Wiberg index values provided the information about the bond order between the two nitrogen atoms of azo group. All these calculations were performed using Gaussian09 suite of program.[46] We have estimated the transition

states and corresponding energy barriers for the *Z-E* isomerization through inversion mechanism.[14, 47] Potential energy surface scan calculations have been performed for obtaining the barriers for rotation mechanism by varying C-N=N-C dihedral angle.[21] Using those rate constants, the Hammett[28] relationship has been plotted for *meta*- and *para*-substituted derivatives. For computations involving solvents, calculations have been performed using polarization continuum model (PCM) and acetonitrile as a solvent.[41]

Experimental section:

General methods:

All the reactions have been carried out with the oven dried glasswares. The reagents (AR or LR grade) and the solvents have been purchased from commercially available sources such as Sigma Aldrich, Merck and TCI etc. Anhydrous solvents for the reactions and for column chromatography have been distilled before use. The NMR spectra have been recorded in Bruker Avance-III 400 MHz NMR spectrometer. ^{1}H and ^{13}C NMR were recorded at operational frequencies 400 MHz and 100 MHz, respectively. For recording the samples, $CDCl_3$, DMSO-d_6, CD_3CN and CD_3OD have been used as the solvents. The chemical shift (δ) values are reported in parts per million (ppm) and the coupling constants (*J*) are reported in Hz. High resolution mass spectra (HRMS) have been recorded using Waters Synapt G2-Si Q-TOF mass spectrometer. HRMS data were obtained from a TOF mass analyser using electrospray ionization (ESI) in both positive and negative modes. Melting points were recorded on SMP20 melting point apparatus, which are uncorrected. IR spectra were recorded on a Bruker Alpha ZnSe ATR FT-IR spectrometer. Column chromatography was performed over silica gel (100–200 mesh). Thin layer chromatography was performed on Merck Silica gel 60 F_{254} TLC plates and

visualized using UV (λ = 254 nm) chamber. The arylazoacetylacetone derivatives **1c-28c**, **29c-30c**, and **33c-37c** have been synthesized as described in the literature.[22] UV-Vis photoswitching and kinetics studies have been performed either using a Cary 5000 or Cary 60 spectrophotometer, whereas the corresponding NMR experiments have been performed in Bruker Avance-III 400 MHz NMR spectrometer. For forward photoswitching (*E-Z* isomerization) samples were irradiated at 365 nm using a LED light source either from Applied Photophysics, SX/LED/360 with an bandwidth 20 nm or a commercial 9W LED light source. The reverse isomerization has been induced by using either a 35 W CFL lamp or a 405 nm LED. The PSS has been established by irradiating the sample for prolonged time such that no further spectral change is observed.

General procedure for synthesis of arylazoacetylacetone derivatives (1-38c):

A mixture of aniline or substituted anilines (20.0 mmol) and deionized water in a two neck round bottom flask was cooled to 0 ºC. To this 37% conc. HCl (6.5 mL) was added and stirred to get a clear solution. Then a cold aqueous solution of sodium nitrite (1.52 g, 22.0 mmol in 20 mL of water) was added dropwise into the reaction mixture slowly. After the addition, the diazonium salt started forming. The reaction mixture was allowed to stir for half an hour for completion. Afterwards, at 0 ºC a cold aqueous solution of sodium acetate (5.90 g, 70.0 mmol) and acetyl acetone (2.00 g, 20.0 mmol in 100 mL of water and 10 ml of ethanol) was added. The reaction was continued at rt and was monitored by TLC. After completion of the reaction, the reaction mixture was filtered off to obtain a yellow-orange solid product, which was dried under vacuum to yield the desired product**.**

General procedure for synthesis of arylazopyrazole derivatives (1-38d):

A mixture of arylazoacetylacetone derivative (1.0 mmol), hydrazine dihydrochloride (2.0 mmol) and Na_2CO_3 (4.0 mmol) in 10 mL absolute ethanol was refluxed. The reaction was followed using TLC upto the completion of the reaction. After completion of the reaction, the product was purified by column chromatography. (Eluent: 1:1 ethylacetate/n-hexane)

Arylazoacetylacetone Derivatives

N-(3-(2-(2,4-dioxopentan-3-ylidene)hydrazinyl)phenyl)acetamide (**28c**):

Yellow-orange solid, mp = 187-189 ^oC, 222.01 mg, 85% yield.^1H NMR (400 MHz, CD_3OD) δ 2.15 (s, 3H), 2.44 (s, 3H), 2.51 (s, 3H), 7.01–7.11 (d, J = 7.3, Hz, 1H), 7.27–7.33 (m, 2H), 7.91 (s, 1H),); ^{13}C NMR (100 MHz, CD_3OD) δ 22.6, 25.3, 30.3, 106.8, 111.4, 116.4, 129.6, 132.8, 140.1, 142.0, 170.4, 197.2, 197.5; HRMS (ESI-TOF): calcd for $C_{13}H_{15}N_3O_3[M-H]^+$: 260.1035; found: 260.1026; IR (ATR, cm^{-1}): 3292, 3078, 1666, 1624, 1596, 876.

3-(2-mesitylhydrazono)pentane-2,4-dione (**31c**):

Yellow solid, mp = 110-111 ^oC, 209.4 mg, 85% yield. ^1H NMR (400 MHz, $CDCl_3$) δ 2.32 (s, 3H), 2.42 (s, 3H), 2.43 (s, 3H), 2.64 (s, 3H), 6.94 (s, 2H), 15.03 (s, 1H); ^{13}C NMR (100 MHz, $CDCl_3$) δ 19.3, 20.9, 27.0, 31.6, 129.8, 130.3, 133.4, 135.7, 136.3, 197.3, 197.5; HRMS (ESI-TOF): calcd for $C_{14}H_{18}N_2O_2[M-H]^+$: 245.1290, found: 245.1278; IR (ATR, cm^{-1}): 2790, 2918, 1714, 1656, 1611.

3-(2-(naphthalen-1-yl)hydrazono)pentane-2,4-dione (**32c**):

Yellow solid, mp = 153-155 °C, 167.89 mg, 66% yield. ^{1}H NMR (400 MHz, $CDCl_3$) δ 2.59 (s, 3H), 2.72 (s, 3H), 7.56–7.66 (m, 3H), 7.75–7.77 (d, *J* = 8.2 Hz, 1H), 7.93–7.95 (d, *J* = 7.9 Hz, 1H), 8.05–8.07 (d, *J* = 8.1 Hz, 1H), 15.78 (s, 1H); ^{13}C NMR (100 MHz, $CDCl_3$) δ 26.8, 31.8, 112.0, 119.6, 123.4, 126.1, 126.1, 126.6, 127.1, 128.8, 134.1, 134.3, 136.5, 197.3, 198.2; HRMS (ESI-TOF): calcd for $C_{15}H_{14}N_2O_2$[M-H]$^+$: 253.0977, found: 253.0965; IR (ATR, cm^{-1}): 3057, 2987, 2921, 1661, 1621, 1494.

3-(2-(3,5-difluorophenyl)hydrazono)pentane-2,4-dione (**38c**):

Yellow solid, mp = 151-153 °C, 237.81 mg, 99% yield. ^{1}H NMR (400 MHz, $CDCl_3$) δ 2.51 (s, 3H), 2.63 (s, 3H), 6.62–6.67 (tt, *J* = 9.1, 2.2 Hz, 1H), 6.93–6.96 (d, *J* = 8.0, 1.9 Hz, 1H), 14.49 (s, 1H); ^{13}C NMR (100 MHz, $CDCl_3$) δ 26.6, 31.8, 99.5 (*J* = 20.3, 9.0 Hz), 100.6 (*J* = 25.7 Hz), 133.9, 144.0, 163.8 (*J* = 247.0, 14.2 Hz), 196.9, 198.5 HRMS (ESI-TOF): calcd for $C_{11}H_{10}F_2N_2O_2$, [M-H]$^+$: 239.0632, found: 239.0620; IR (ATR, cm^{-1}): 3059, 1675, 1602, 1524, 1471, 1407.

Arylazopyrazole Derivatives

(E)-3,5-dimethyl-4-(phenyldiazenyl)-1*H*-pyrazole (**1d**):

Yellow solid, mp = 141-143 °C, 170.2 mg, 85% yield. ^{1}H NMR (400 MHz, $CDCl_3$) δ 2.64 (s, 6H), 7.41-7.43 (m, 1H), 7.78-7.52 (t, *J* = 7.2 Hz, 2H), 7.82-7.84 (m, 2H); ^{13}C NMR (100 MHz, $CDCl_3$) δ 12.2, 121.9, 128.9, 129.5, 134.7, 141.5, 153.6; HRMS (ESI-TOF): calcd for $C_{11}H_{12}N_4$ [M+H]$^+$: 201.1140, found: 201.1132; IR (ATR, cm^{-1}): 3114, 3042, 2968, 2887, 1411, 1322, 1118, 829.

(*E*)-4-((2-fluorophenyl)diazenyl)-3,5-dimethyl-1*H*-pyrazole (**2d**):

Yellow solid, mp = 158-160 ºC, 209.5 mg, 96% yield. ^{1}H NMR (400 MHz, $CDCl_3$) δ 2.63 (s, 6H), 7.35-7.43 (m, 2H), 7.69-7.72 (dt, *J* = 7.7, 1.7 Hz, 1H), 7.78-7.79 (t, *J* = 1.7 Hz, 1H); ^{13}C NMR (100 MHz, $CDCl_3$) δ 12.3, 120.9, 121.3, 129.2, 130.0, 134.7, 134.9, 141.8, 154.4; HRMS (ESI-TOF) calcd for $C_{11}H_{11}FN_4$ $[M+H]^+$: 219.1046, found: 219.1038; IR (ATR, cm^{-1}): 3173, 3110, 2966, 2883, 1400, 1315, 1184, 776.

(*E*)-4-((3-fluorophenyl)diazenyl)-3,5-dimethyl-1*H*-pyrazole (**3d**):

Yellow solid, mp = 128-131 ºC, 178.9 mg, 82% yield. ^{1}H NMR (400 MHz, $CDCl_3$) δ 2.64 (s, 6H), 7.09-7.13 (tdd, *J* = 8.2, 2.6, 0.7 Hz, 1H), 7.42-7.51 (m, 2H), 7.63-7.65 (dt, *J* = 6.8, 1.4 Hz, 1H); ^{13}C NMR (100 MHz, $CDCl_3$) δ 12.2, 107.0 (d, *J* = 22.7 Hz), 116.2 (d, *J* = 22.1 Hz), 119.5 (d, *J* = 2.8 Hz), 130.1 (d, *J* = 8.6 Hz), 134.6, 141.9, 155.1 (d, *J* = 6.8 Hz), 163.4 (d, *J* = 245.1 Hz); HRMS (ESI-TOF) calcd for $C_{11}H_{11}FN_4$ $[M+H]^+$: 219.1046, found: 219.1035; IR (ATR, cm^{-1}): 3198, 3115, 3051, 2965, 2896, 1666, 1408, 1324, 1108, 867.

(*E*)-4-((4-fluorophenyl)diazenyl)-3,5-dimethyl-1*H*-pyrazole (**4d**):

Yellow solid, mp = 166-168 ºC, 202.9 mg, 93% yield. ^{1}H NMR (400 MHz, $CDCl_3$) δ 2.63 (s, 6H), 7.15-7.19(t, *J* = 8.6 Hz, 2H), 7.80-7.84 (dd, *J* = 8.6, 5.2 Hz, 2H); ^{13}C NMR (100 MHz, $CDCl_3$) δ 12.2, 115.8 (d, *J* = 22.8 Hz), 123.6 (d, *J* = 8.7 Hz), 134.5, 141.5, 150.0 (d, *J* = 2.9 Hz), 163.5 (d, *J* = 247.9 Hz); HRMS (ESI-TOF) calcd for $C_{11}H_{11}FN_4$ $[M+H]^+$: 219.1046, found: 219.1057; IR (ATR, cm^{-1}): 3605, 2385, 2308, 1421, 1218, 831.

(*E*)-4-((2-chlorophenyl)diazenyl)-3,5-dimethyl-1*H*-pyrazole (**5d**):

Yellow solid, mp = 170-172 ºC, 143.2 mg, 61% yield. ^{1}H NMR (400 MHz, $CDCl_3$) δ 2.67 (s, 6H), 7.31-7.34 (m, 2H), 7.53-7.55 (m, 1H), 7.69-7.72 (m, 1H); ^{13}C NMR (100 MHz, $CDCl_3$) δ 12.3, 116.8, 127.1, 130.2, 130.4, 134.3, 135.6, 142.1, 149.4; HRMS (ESI-TOF) calcd for $C_{11}H_{11}ClN_4$ $[M+H]^+$: 235.0750, found: 235.0741; IR (ATR, cm^{-1}): 3192, 3113, 3052, 2914, 1491, 1395, 1194, 889.

(*E*)-4-((3-chlorophenyl)diazenyl)-3,5-dimethyl-1*H*-pyrazole (**6d**):

Yellow solid, mp = 170-172 ºC, 164.3 mg, 70% yield. ^{1}H NMR (400 MHz, $CDCl_3$) δ 2.65 (s, 6H), 7.18-7.26 (m, 2H), 7.34-7.40 (m, 1H), 7.69-7.73 (td, J = 1.8, 7.9 Hz 1H); ^{13}C NMR (100 MHz, $CDCl_3$) δ 12.2, 116.8 (d, J = 19.7 Hz), 117.1, 124.1 (d, J = 3.8 Hz), 130.7 (d, J = 8.0 Hz), 135.5, 141.4 (d, J = 7.0 Hz), 141.9, 159.4 (d, J = 25.4 Hz); HRMS (ESI-TOF) calcd for $C_{11}H_{11}ClN_4$ $[M+H]^+$: 235.0750, found: 235.0741; IR (ATR, cm^{-1}): 2984, 1502, 1359, 1303, 1177, 1063, 922, 767, 680.

(*E*)-4-((4-chlorophenyl)diazenyl)-3,5-dimethyl-1*H*-pyrazole (**7d**):

Yellow solid, mp = 167-169 ºC, 218.3 mg, 93% yield. ^{1}H NMR (400 MHz, $CDCl_3$) δ 2.62 (s, 6H), 7.43-7.46 (d, J = 8.7 Hz, 2H), 7.73-7.77 (d, J = 8.7 Hz, 2H); ^{13}C NMR (100 MHz, $CDCl_3$) δ 12.22, 123.10, 129.12, 134.67, 135.18, 141.73, 151.88; HRMS (ESI-TOF) calcd for $C_{11}H_{11}ClN_4$ $[M+H]^+$: 235.0750, found: 235.0759; IR (ATR, cm^{-1}): 3192, 2957, 2875, 2820, 1506, 1412, 829.

(*E*)-4-((2-bromophenyl)diazenyl)-3,5-dimethyl-1*H*-pyrazole (**8d**):

Yellow solid, mp = 165-168 ºC, 195.4 mg, 70% yield. ^{1}H NMR (400 MHz, $CDCl_3$) δ 2.68 (s, 6H), 7.23-7.27 (t, *J* = 7.2 Hz, 1H), 7.36-7.40 (t, *J* = 7.5 Hz, 1H), 7.68-7.70 (d, *J* = 7.4 Hz, 1H), 7.73-7.75 (d, *J* = 7.9 Hz, 1H); ^{13}C NMR (100 MHz, $CDCl_3$) δ 12.4, 117.1, 124.8, 127.8, 130.5, 133.5, 135.5, 142.1, 150.4; ; HRMS (ESI-TOF) calcd for $C_{11}H_{11}BrN_4$ $[M+H]^+$: 279.0245, 281.0225, found: 279.0236, 281.0209; IR (ATR, cm^{-1}): 3194, 3105, 3051, 2966, 2915, 1498, 1405, 854.

(*E*)-4-((3-bromophenyl)diazenyl)-3,5-dimethyl-1*H*-pyrazole (**9d**):

Yellow solid, mp = 168-170 ºC, 251.2 mg, 90% yield. ^{1}H NMR (400 MHz, $CDCl_3$) δ 2.63 (s, 6H), 7.34-7.38 (t, *J* = 7.9 Hz, 1H), 7.51-7.53 (ddd, *J* = 7.9, 1.9, 0.9 Hz, 1H), 7.74-7.76 (ddd, *J* = 7.5, 1.7, 0.7 Hz, 1H), 7.93-7.94 (t, *J* = 1.8 Hz, 1H); ^{13}C NMR (100 MHz, $CDCl_3$) δ 12.3, 121.8, 123.0, 123.8, 130.3, 132.1, 135.0, 142.1, 154.5; HRMS (ESI-TOF) calcd for $C_{11}H_{11}BrN_4$ $[M+H]^+$: 279.0245, 281.0225, found: 279.0232, 281.0208; IR (ATR, cm^{-1}): 3176, 3114, 2965, 2921, 1495, 1393, 1312, 901, 773.

(*E*)-4-((4-bromophenyl)diazenyl)-3,5-dimethyl-1*H*-pyrazole (**10d**):

Yellow solid, mp = 166-168 ºC, 201.1 mg, 72% yield. ^{1}H NMR (400 MHz, $CDCl_3$) δ 2.61 (s, 6H), 7.60-7.62 (d, *J* = 8.8 Hz, 2H), 7.68-7.71 (d, *J* = 8.8 Hz, 2H); ^{13}C NMR (100 MHz, $CDCl_3$) δ 12.2, 123.4, 123.6, 132.1, 134.7, 141.7, 152.2; HRMS (ESI-TOF) calcd for $C_{11}H_{11}BrN_4$ $[M+H]^+$: 279.0245, 281.0225, found: 279.0235, 281.0211; IR (ATR, cm^{-1}): 3194, 3103, 2961, 2879, 1415, 827, 774.

(*E*)-2-((3,5-dimethyl-1*H*-pyrazol-4-yl)diazenyl)phenol (**11d**):

Yellow solid, mp = 164-166 ºC, 201.1 mg, 93% yield. ^{1}H NMR (400 MHz, $CDCl_3$) δ 2.60 (s, 6H), 6.99-7.06 (m, 2H), 7.27-7.31 (td, *J* = 6.0, 1.5 Hz, 1H), 7.80-7.83 (dd, *J* = 7.9, 1.6,Hz, 1H); ^{13}C NMR (100 MHz, $CDCl_3$) δ 12.3, 117.9 119.8, 131.5, 131.6, 132.5, 137.6, 140.9, 152.1; HRMS (ESI-TOF) calcd for $C_{11}H_{12}N_4O$ $[M+H]^+$: 217.1089, found: 217.1077; IR (ATR, cm^{-1}): 3281, 3116, 2914, 2807, 1418, 1221, 820.

(*E*)-3-((3,5-dimethyl-1*H*-pyrazol-4-yl)diazenyl)phenol (**12d**):

Yellow solid, mp = 199-203 ºC, 198.9 mg, 92% yield. ^{1}H NMR (400 MHz, DMSO-d_6) δ 2.39 (s, 3H), 2.50 (s, 3H), 6.82-6.84 (dd, *J* = 8.0, 1.3 Hz, 1H), 7.13 (1H), 7.19-7.21 (d, *J* = 7.8 Hz, 1H), 7.28-7.32 (t, *J* = 7.9 Hz, 1H), 9.68 (s, 1H, OH), 12.85 (s, 1H, NH); ^{13}C NMR (100 MHz, DMSO-d_6): δ 10.5, 14.2, 106.8, 114.5, 117.1, 130.3, 134.5, 138.8, 143.0, 154.8, 158.5; HRMS (ESI-TOF) calcd for $C_{11}H_{12}N_4O$ $[M+H]^+$: 217.1089, found: 217.1080; IR (ATR, cm^{-1}): 3335, 3246, 3060, 2922, 1590, 1470, 1411, 1128, 1114, 857.

(*E*)-4-((3,5-dimethyl-1*H*-pyrazol-4-yl)diazenyl)phenol (**13d**):

Yellow solid, mp = 198-205 ºC, 170.8 mg, 79% yield. ^{1}H NMR (400 MHz, DMSO-d_6) δ 2.40 (s, 3H), 2.46 (s, 3H), 6.86-6.89 (d, *J* = 8.9 Hz, 2H), 7.61-7.63 (d, *J* = 8.9 Hz, 2H), 9.97 (s, 1H, OH), 12.72 (s, 1H, NH); ^{13}C NMR (100 MHz, DMSO-d_6) δ 10.4, 14.1, 116.1, 123.6, 134.2, 137.7, 142.9, 146.6, 159.5; HRMS (ESI-TOF) calcd

for $C_{11}H_{12}N_4O$ $[M+H]^+$: 217.1089, found: 217.1081; IR (ATR, cm^{-1}): 3291, 3190, 3119, 2917, 1482, 1420, 1134, 1061, 825.

(*E*)-3,5-dimethyl-4-((2-(trifluoromethyl)phenyl)diazenyl)-1*H*-pyrazole (**14d**):

Yellow solid, mp = 170-172 ºC, 193.1 mg, 72% yield. ^{1}H NMR (400 MHz, $CDCl_3$) δ 2.65 (s, 6H), 7.46-7.50 (t, *J* = 7.8 Hz,1H), 7.60-7.64 (t, *J* = 7.9 Hz, 1H), 7.79-7.81 (d, *J* = 8.0 Hz, 2H); ^{13}C NMR (100 MHz, $CDCl_3$) δ 12.1, 115.8, 124.2 (q, *J* = 273.7 Hz), 126.3 (q, *J* = 5.5 Hz), 127.3 (q, *J* = 30.7 Hz), 128.9, 132.4, 135.5, 142.4, 150.4; HRMS (ESI-TOF) calcd for $C_{12}H_{11}F_3N_4$ $[M+H]^+$: 269.1014, found: 269.1002; IR (ATR, cm^{-1}): 3196, 3107, 3049, 2883, 2308, 1497, 1408, 1122, 1035, 762.

(*E*)-3,5-dimethyl-4-((3-(trifluoromethyl)phenyl)diazenyl)-1*H*-pyrazole (**15d**):

Yellow solid, mp = 153-155 ºC, 198.5 mg, 74% yield. ^{1}H NMR (400 MHz, $CDCl_3$) δ 2.66 (s, 6H), 7.55-7.59 (t, *J* = 7.8 Hz, 1H), 7.63-7.65 (d, *J* = 7.7 Hz, 1H), 7.95-7.97 (d, *J* = 7.9 Hz, 1H), 8.05 (s, 1H); ^{13}C NMR (100 MHz, $CDCl_3$) δ 12.2, 118.8 (q, *J* = 3.8 Hz), 124.0 (q, *J* = 272.04 Hz), 124.9, 125.71 (q, *J* = 3.7 Hz), 129.5, 131.42 (q, *J* = 32.6 Hz), 134.7, 142.0, 153.5; HRMS (ESI-TOF) calcd for $C_{12}H_{11}F_3N_4$ $[M+H]^+$: 269.1014, found 269.1004; IR (ATR, cm^{-1}): 3201, 3126, 2958, 2916, 1488, 1319, 1106, 787, 689.

(*E*)-3,5-dimethyl-4-((4-(trifluoromethyl)phenyl)diazenyl)-1*H*-pyrazole (**16d**):

Yellow solid, mp = 138-140 ºC, 222.6 mg, 83% yield. ^{1}H NMR (400 MHz, $CDCl_3$) δ 2.65 (s, 6H), 7.70-7.72 (d, *J* = 8.3 Hz, 2H), 7.84-7.86 (d, *J* = 8.2 Hz, 2H); ^{13}C NMR (100 MHz, $CDCl_3$) δ 12.2, 122.0, 124.1 (q, *J* = 272 Hz), 126.1 (q, *J* = 3.4 Hz), 130.8 (q, *J* = 32.4 Hz), 134.9, 142.1, 155.4, 155.4; HRMS (ESI-TOF) calcd for $C_{12}H_{11}F_3N_4$

$[M+H]^+$: 269.1014, found 269.1001; IR (ATR, cm^{-1}): 3197, 3109, 2973, 2890, 1673, 1416, 1317, 1113, 895, 840.

(*E*)-4-((2-methoxyphenyl)diazenyl)-3,5-dimethyl-1*H*-pyrazole (**17d**):

Yellow solid, mp = 156-159 ºC, 161.2 mg, 70% yield. ^{1}H NMR (400 MHz, $CDCl_3$) δ 2.66 (s, 6H), 4.01 (s, 3H, OCH_3), 7.01-7.05 (td, *J* = 7.6, 1.1 Hz, 1H), 7.07-7.09 (dd, *J* = 8.3, 0.7 Hz, 1H), 7.36-7.40 (td, *J* = 8.5, 1.7 Hz, 1H), 7.62-7.64 (dd, *J* = 7.9, 1.6 Hz, 1H); ^{13}C NMR (100 MHz, $CDCl_3$) δ 12.1, 56.47, 112.8, 116.3, 120.9, 130.8, 135.7, 141.3, 143.2, 156.2; HRMS (ESI-TOF) calcd for $C_{12}H_{14}N_4O$ $[M+H]^+$: 231.1246, found: 231.1235; IR (ATR, cm^{-1}): 3193, 3109, 3042, 2877, 2826, 2308, 1586, 1408, 1110, 892.

(*E*)-4-((3-methoxyphenyl)diazenyl)-3,5-dimethyl-1*H*-pyrazole (**18d**):

Yellow solid, mp = 144-145 ºC, 225.7 mg, 98% yield. ^{1}H NMR (400 MHz, $CDCl_3$) δ 2.66 (s, 6H), 3.91 (s, 3H, OCH_3), 6.97-7.00 (ddd, *J* = 8.0, 2.6, 1.1 Hz, 1H), 7.37-7.47 (m, 3H); ^{13}C NMR (100 MHz, $CDCl_3$) δ 12.2, 55.4, 105.5, 115.7, 115.8, 129.7, 134.6, 141.5, 154.8, 160.2; HRMS (ESI-TOF) calcd for $C_{12}H_{14}N_4O$ $[M+H]^+$: 231.1246, found: 231.1235; IR (ATR, cm^{-1}): 3120, 3045, 2957, 2897, 1737, 1475, 1404, 1133, 834, 675.

(*E*)-4-((4-methoxyphenyl)diazenyl)-3,5-dimethyl-1*H*-pyrazole (**19d**):

Yellow solid, mp = 174-177 ºC, 200.3 mg, 87% yield. ^{1}H NMR (400 MHz, $CDCl_3$) δ 2.62 (s, 6H), 3.90 (s, 3H, OCH_3), 6.99-7.01 (d, *J* = 9.0 Hz, 2H), 7.80-7.82 (d, *J* = 9.0 Hz, 2H); ^{13}C NMR (100 MHz, $CDCl_3$) δ 12.2, 55.5, 114.0, 123.4, 134.5, 141.0, 147.9,

160.8; HRMS (ESI-TOF) calcd for $C_{12}H_{14}N_4O$ $[M+H]^+$: 231.1246, found: 231.1250; IR (ATR, cm^{-1}): 3740, 2921, 2544, 1494, 1412, 1144, 1016, 832, 770.

(*E*)-3,5-dimethyl-4-((2-nitrophenyl)diazenyl)-1*H*-pyrazole (**20d**):

Orange solid, mp = 170-172 ºC, 198.6 mg, 81% yield. ^{1}H NMR (400 MHz, $CDCl_3$) δ 2.60 (s, 6H), 7.47-7.51 (td, *J* = 7.6, 1.3 Hz, 1H), 7.61-7.66 (td, *J* = 7.2, 1.3 Hz, 1H), 7.70-7.73 (dd, *J* = 8.1, 1.2 Hz, 1H), 7.82-7.84 (dd, *J* = 8.0, 1.1 Hz, 1H), 11.87 (br, 1H, NH); ^{13}C NMR (100 MHz, $CDCl_3$) δ 12.2, 118.0, 123.7, 129.1, 132.6, 135.5, 142.8, 145.9, 147.4; HRMS (ESI-TOF) calcd for $C_{11}H_{11}N_5O_2$ $[M+H]^+$: 246.0991, found: 246.0994; IR (ATR, cm^{-1}): 3192, 2886, 1588, 1519, 1406, 1110, 848, 757.

(*E*)-3,5-dimethyl-4-((3-nitrophenyl)diazenyl)-1*H*-pyrazole (**21d**):

Orange solid, mp = 227-229 ºC, 203.5 mg, 83% yield. ^{1}H NMR (400 MHz, $CDCl_3$) δ 2.64 (s, 6H), 7.65-7.69 (t, *J* = 8.0 Hz, 1H), 8.14-8.16 (d, *J* = 7.9 Hz, 1H), 8.25-8.27 (d, *J* = 8.0 Hz, 1H), 8.62 (s, 1H); ^{13}C NMR (100 MHz, $CDCl_3$) δ 12.4, 116.2, 123.5, 128.24, 129.7, 134.9, 143.2, 149.0, 154.0; HRMS (ESI-TOF) calcd for $C_{11}H_{11}N_5O_2$ $[M+H]^+$: 246.0991, found: 246.0979; IR (ATR, cm^{-1}): 3185, 3096, 2967, 2881, 2823, 1412, 1340, 865, 803.

(*E*)-3,5-dimethyl-4-((4-nitrophenyl)diazenyl)-1*H*-pyrazole (**22d**):

Orange solid, mp = 198-200 ºC, 237.8 mg, 97% yield.^{1}H NMR (400 MHz, $CDCl_3$) δ 2.65 (s, 6H), 7.90-7.93 (d, *J* = 8.8 Hz, 2H), 8.34-8.37 (d, *J* = 8.8 Hz, 2H); ^{13}C NMR (100 MHz, $CDCl_3$) δ 12.3, 122.4, 124.7, 135.4, 143.0, 147.7, 156.9; HRMS (ESI-

TOF) calcd for $C_{11}H_{11}N_5O_2$ $[M+H]^+$: 246.0991, found: 246.0980; IR (ATR, cm^{-1}): 3195, 3101, 2969, 2886, 1507, 1400, 898, 849.

(*E*)-3,5-dimethyl-4-(*o*-tolyldiazenyl)-1*H*-pyrazole (**23d**):

Yellow solid, mp = 163-165 ºC, 207.5 mg, 95% yield.^{1}H NMR (400 MHz, $CDCl_3$) δ 2.67 (s, 6H), 2.68 (s, 3H), 7.26-7.36 (m, 3H), 7.64-7.67 (dd, *J* = 7.3, 1.4 Hz, 1H); ^{13}C NMR (100 MHz, $CDCl_3$) δ 12.3, 17.9, 114.7, 126.3, 129.5, 131.1, 135.4, 136.8, 141.4, 151.5; HRMS (ESI-TOF) calcd for $C_{12}H_{14}N_4$ $[M+H]^+$: 215.1297, found: 215.1290; IR (ATR, cm^{-1}): 3193, 3109, 3042, 2877, 2826, 2308, 1586, 1494, 1408, 892, 820, 763.

(*E*)-3,5-dimethyl-4-(*m*-tolyldiazenyl)-1*H*-pyrazole (**24d**):

Yellow solid, mp = 148-152 ºC, 205.7 mg, 96% yield. ^{1}H NMR (400 MHz, $CDCl_3$) δ 2.47 (s, 3H), 2.65 (s, 6H), 7.22-7.24 (d, *J* = 7.5 Hz, 1H), 7.36-7.40 (t, *J* = 8.4 Hz, 1H), 7.62-7.64 (m, 2H); ^{13}C NMR (100 MHz, $CDCl_3$) δ 12.2, 21.4, 119.1, 122.4, 128.7, 130.3, 134.8, 138.8, 141.5, 153.6; HRMS (ESI-TOF) calcd for $C_{12}H_{14}N_4$ $[M+H]^+$: 215.1297, found: 215.1310; IR (ATR, cm^{-1}): 3193, 3102, 3043, 2954, 2918, 1595, 1497, 1480, 1404, 842, 782.

(*E*)-3,5-dimethyl-4-(*p*-tolyldiazenyl)-1*H*-pyrazole (**25d**):

Yellow solid, mp = 153-155 ºC, 197.1 mg, 92% yield. ^{1}H NMR (400 MHz, $CDCl_3$) δ 2.44 (s, 3H), 2.63 (s, 6H), 7.28-7.30 (d, *J* = 8.2 Hz, 2H), 7.72-7.74 (d, *J* = 8.2 Hz, 2H); ^{13}C NMR (100 MHz, $CDCl_3$) δ 12.2, 21.4, 121.8, 129.6, 134.6, 139.8, 141.6,

151.6; HRMS (ESI-TOF) calcd for $C_{12}H_{14}N_4$ $[M+H]^+$: 215.1297, found: 215.1288; IR (ATR, cm^{-1}): 3195, 3113, 3041, 2874, 2820, 2310, 1591, 1409, 816, 770.

(*E*)-3-((3,5-dimethyl-1*H*-pyrazol-4-yl)diazenyl)benzoic acid (**26d**):

Yellow solid, mp = 230-233 °C, 136.8 mg, 56% yield. ^{1}H NMR (400 MHz, CD_3OD) δ 2.55 (s, 6H), 7.47-7.50 (t, *J* = 7.7 Hz, 1H), 7.82-7.84 (d, *J* = 7.8 Hz, 1H), 8.00-8.02 (d, *J* = 7.5 Hz, 1H), 8.39 (s, 1H); ^{13}C NMR (100 MHz, CD_3OD) δ 10.6, 122.3, 122.9, 128.0, 129.9, 134.2, 138.9, 141.2, 153.3, 173.5; HRMS (ESI-TOF) calcd for $C_{12}H_{12}N_4O_2$ $[M+H]^+$: 245.1039, found: 245.1030; IR (ATR, cm^{-1}): 3736, 3207, 2918, 2388, 1677, 1368, 1269, 1164, 1062, 864, 764.

(*E*)-4-((3,5-dimethyl-1*H*-pyrazol-4-yl)diazenyl)benzoic acid (**27d**):

Yellow solid, mp = 219-223 °C, 197.8 mg, 81% yield. ^{1}H NMR (400 MHz, DMSO-d_6) δ 2.47 (s, 6H), 7.78-7.81 (d, *J* = 8.4 Hz, 2H), 8.06-8.08 (d, *J* = 8.4 Hz, 2H), 13.00 (br, 1H); ^{13}C NMR (100 MHz, DMSO-d_6) δ 12.5, 121.8, 131.0, 131.4, 135.1, 141.6, 156.0, 167.4; HRMS (ESI-TOF) calcd for $C_{12}H_{12}N_4O_2$ $[M+H]^+$: 245.1039, found: 245.1030; IR (ATR, cm^{-1}): 3737, 3199, 2923, 2314, 1407, 1292, 1061, 996, 767.

(*E*)-N-(3-((3,5-dimethyl-1*H*-pyrazol-4-yl)diazenyl)phenyl)acetamide (**28d**):

Yellow solid, mp = 209-212 °C, 146.7 mg, 57% yield.^{1}H NMR (400 MHz, DMSO-d_6) δ 2.07 (s, 3H, $NHCOCH_3$), 2.40 (s, 3H), 2.51 (s, 3H), 7.41-7.43 (m, 2H), 7.62-7.65 (m, 1H), 7.98 (s, 1H), 10.12 (br, 1H), 12.87 (br, 1H); ^{13}C NMR (100 MHz, DMSO-d_6) δ 10.5, 14.2, 24.5, 111.9, 117.1, 120.3, 129.8, 134.5, 139.0, 140.6, 143.0, 153.8,

169.0; HRMS (ESI-TOF) calcd for $C_{13}H_{15}N_5O$ $[M+H]^+$: 258.1355, found: 258.1367; IR (ATR, cm^{-1}): 3390, 3307, 3198, 3138, 2918, 1659, 1548, 1493, 1428, 885.

(*E*)-N-(4-((3,5-dimethyl-1*H*-pyrazol-4-yl)diazenyl)phenyl)acetamide (**29d**):

Yellow solid, mp = 222-225 ºC, 239.2 mg, 93% yield. ^{1}H NMR (400 MHz, DMSO-d_6) δ 2.08 (s, 3H), 2.42 (s, 3H), 2.47 (s, 3H), 7.68-7.74 (dd, *J* = 8.9, 7.9 Hz, 4H), 10.18 (s, 1H), 12.78 (s, 1H); ^{13}C NMR (100 MHz, DMSO-d_6) δ 24.6, 119.6, 122.6, 134.4, 141.0, 149.0, 169.0; HRMS (ESI-TOF) calcd for $C_{13}H_{15}N_5O$ $[M+H]^+$: 258.1355, found: 258.1343; IR (ATR, cm^{-1}): 3266, 3176, 3088, 3039, 2958, 2871, 2310, 1659, 1598, 1531, 1419, 836.

(*E*)-4-((2-ethylphenyl)diazenyl)-3,5-dimethyl-1*H*-pyrazole (**30d**):

Yellow solid, mp = 154-156 ºC, 226.0 mg, 99% yield. ^{1}H NMR (400 MHz, $CDCl_3$) δ 1.30-1.34(t, *J* = 7.5 Hz, 3H), 2.65 (s, 6H), 3.08-3.14 (q, *J* = 7.5 Hz, 2H), 7.26-7.30 (m, 1H), 7.35-7.36 (m, 2H), 7.64-7.66 (d, *J* = 7.8 Hz, 1H); ^{13}C NMR (100 MHz, $CDCl_3$) δ 12.26, 16.21, 24.95, 114.70, 126.40, 129.60, 129.78, 135.37, 141.42, 142.80, 150.93; HRMS (ESI-TOF) calcd for $C_{13}H_{16}N_4$ $[M+H]^+$: 229.1453, found: 229.1444; IR (ATR, cm^{-1}): 3199, 3116, 3047, 2873, 2311, 1406, 1322, 1113, 839, 762.

(*E*)-4-(mesityldiazenyl)-3,5-dimethyl-1*H*-pyrazole (**31d**):

Yellow solid, mp = 168-170 ºC, 239.8 mg, 99% yield. ^{1}H NMR (400 MHz, $CDCl_3$) δ 2.34 (s, 3H), 2.39 (s, 6H), 2.58 (s, 6H), 6.95 (s, 2H); ^{13}C NMR (100 MHz, $CDCl_3$) δ 12.2, 19.6, 21.0, 129.9, 130.9, 135.3, 137.3, 149.4; HRMS (ESI-TOF) calcd for

$C_{14}H_{18}N_4$ $[M+H]^+$: 243.1610, found: 243.1599; IR (ATR, cm^{-1}): 3194, 3110, 3043, 2955, 2879, 2312, 1419, 846.

(*E*)-3,5-dimethyl-4-(naphthalen-1-yldiazenyl)-1*H*-pyrazole (**32d**):

Yellow solid, mp = 180-182 ºC, 157.7 mg, 63% yield. ^{1}H NMR (400 MHz, $CDCl_3$) δ 2.77 (s, 6H), 7.55-7.67 (m, 3H), 7.80-7.82 (dd, *J* = 7.5, 0.8 Hz, 1H), 7.92-7.95 (dd, *J* = 7.9, 3.5 Hz, 2H), 8.82-8.84 (d, *J* = 8.4 Hz, 1H); ^{13}C NMR (100 MHz, $CDCl_3$) δ 12.6, 110.8, 123.5, 125.7, 126.2, 126.5, 127.9, 129.8, 131.0, 134.3, 135.9, 141.6, 148.7; HRMS (ESI-TOF) calcd for $C_{15}H_{14}N_4$ $[M+H]^+$: 251.1297, found: 251.1307; IR (ATR, cm^{-1}): 3177, 3112, 3042, 2964, 2923, 2877, 2309, 1412, 965, 765.

(*E*)-4-((2,5-dichlorophenyl)diazenyl)-3,5-dimethyl-1*H*-pyrazole (**33d**):

Yellow solid, mp = 238-242 ºC, 121.1 mg, 45% yield. ^{1}H NMR (400 MHz, DMSO-d_6) δ 2.42 (s, 3H), 2.53 (s, 3H), 7.47-7.49 (dd, *J* = 8.6, 1.8 Hz, 1H), 7.62 (d, *J* = 0.4 Hz, 1H), 7.65-7.68 (d, *J* = 8.6 Hz, 1H), 13.06 (s, 1H); ^{13}C NMR (100 MHz, DMSO-d_6) δ 10.55, 14.30, 116.84, 130.30, 131.60, 132.34, 133.10, 135.66, 140.86, 143.60, 149.83; HRMS (ESI-TOF) calcd for $C_{11}H_{10}Cl_2N_4$ $[M+H]^+$: 269.0361, found: 269.0351; IR (ATR, cm^{-1}): 3201, 3112, 3044, 2957, 2870, 1415, 1367, 1335, 882, 836, 768, 708.

(*E*)-4-((2,6-dichlorophenyl)diazenyl)-3,5-dimethyl-1H-pyrazole (**34d**):

Yellow solid, mp = 178-181 ºC, 239.5 mg, 89% yield. ^{1}H NMR (400 MHz, $CDCl_3$) δ 2.64 (s, 6H), 7.13-7.18 (dd, *J* = 8.4, 7.8 Hz, 1H), 7.40-7.42 (d, *J* = 8.0 Hz, 2H); ^{13}C

NMR (100 MHz, $CDCl_3$) δ 12.2, 127.2, 127.6, 129.1, 135.4, 142.4, 148.7; HRMS (ESI-TOF) calcd for $C_{11}H_{10}Cl_2N_4$ $[M+H]^+$: 269.0361, found: 269.0353; IR (ATR, cm^{-1}): 3188, 3089, 2958, 2881, 2821, 2310, 1405, 1327, 1256, 893, 771.

(*E*)-4-((2,4-difluorophenyl)diazenyl)-3,5-dimethyl-1*H*-pyrazole (**35d**):

Yellow solid, mp = 185-187 ºC, 184.3 mg, 78% yield. ^1H NMR (400 MHz, $CDCl_3$) δ 2.63 (s, 6H), 6.91-7.00 (m, 2H), 7.70-7.76 (m, 1H); ^{13}C NMR (100 MHz, $CDCl_3$) δ 12.2, 104.5 (*J* = 25.5 Hz), 111.5 (*J* = 22.4 Hz), 118.1 (*J* = 9.8 Hz), 138.3 (*J* = 4.0 Hz), 141.9, 159.6 (*J* = 216.8, 4.6 Hz), 163.4 (*J* = 246.1, 11.4 Hz); HRMS (ESI-TOF) calcd for $C_{11}H_{10}F_2N_4$ $[M+H]^+$: 237.0952, found: 237.0941; IR (ATR, cm^{-1}): 3430, 3198, 3108, 2882, 2312, 1404, 1261, 961, 848.

(*E*)-4-((2,5-difluorophenyl)diazenyl)-3,5-dimethyl-1*H*-pyrazole (**36d**):

Yellow solid, mp = 196 -198 ºC, 127.6 mg, 54% yield. ^1H NMR (400 MHz, $CDCl_3$) δ 2.63 (s, 6H), 7.04-7.10 (m, 1H), 7.17-7.23 (td, *J* = 9.3, 4.6 Hz, 1H), 7.41-7.46 (m, 1H); ^{13}C NMR (100 MHz, $CDCl_3$) δ 12.2, 103.4 (*J* = 24.9 Hz), 116.9 (*J* = 25.0, 8.1 Hz), 117.6 (*J* = 22.5, 8.5 Hz), 135.4, 141.9 (*J* = 5.9, 2.8 Hz), 142.3, 155.7 (*J* = 250.3, 2.4 Hz), 158.9 (*J* = 242.3, 2.3 Hz); HRMS (ESI-TOF) calcd for $C_{11}H_{10}F_2N_4$ $[M+H]^+$: 237.0952, found: 237.0944; IR (ATR, cm^{-1}): 3192, 3113, 2876, 2819, 2310, 1388, 1240, 869, 725.

(*E*)-4-((2,6-difluorophenyl)diazenyl)-3,5-dimethyl-1*H*-pyrazole (**37d**):

Yellow solid, mp = 145-148 ºC, 125.2 mg, 53% yield. ^{1}H NMR (400 MHz, $CDCl_3$) δ 2.61 (s, 6H), 7.00-7.04 (m, 2H), 7.22-7.28 (m, 1H); ^{13}C NMR (100 MHz, $CDCl_3$) δ 12.2, 112.3 (*J* = 18.2, 5.6 Hz), 128.5 (*J* = 10.1 Hz), 132.0, 136.2, 142.1, 155.7 (*J* = 255.2, 4.8 Hz); HRMS (ESI-TOF) calcd for $C_{11}H_{10}F_2N_4$ $[M+H]^+$: 237.0952, found: 237.0941; IR (ATR, cm^{-1}): 3204, 2971, 2913, 2301, 1405, 1233, 1014, 774.

(*E*)-4-((3,5-difluorophenyl)diazenyl)-3,5-dimethyl-1*H*-pyrazole (**38d**):

Yellow solid, mp = 185-190 ºC, 205.5 mg, 87% yield. ^{1}H NMR (400 MHz, $CDCl_3$) δ 2.62 (s, 6H), 6.83-6.87 (tt, *J* = 8.5, 2.4 Hz, 1H), 7.33-7.35 (m, 2H); ^{13}C NMR (100 MHz, $CDCl_3$) δ 12.3, 104.3 (*J* = 26.0 Hz), 105.0 (*J* = 19.3, 7.0 Hz), 134.5, 142.4, 155.6 (*J* = 9.0 Hz), 163.3 (*J* = 246.1, 13.2 Hz); HRMS (ESI-TOF) calcd for $C_{11}H_{10}F_2N_4$ $[M+H]^+$: 237.0952, found: 237.0942; IR (ATR, cm^{-1}): 3193, 3098, 3046, 2878, 2822, 1406, 1256, 856, 770, 657.

General procedure of synthesis of (*E*)-1,3,5-trimethyl-4-(phenyldiazenyl)-1*H*-pyrazole Derivatives:

A mixture of arylazopyrazole (1.0 mmol) and 1 ml of DMSO was taken in a round bottom flask. To this solution, pulverized potassium hydroxide (3.0 mmol) was added and the resulting suspension was stirred for 1 h at 80 °C. Then cooled to room temperature, and then methyl iodide (1.2 mmol) in 1 ml of DMSO was added over a period of 1 h at 20 °C . The mixture was then allowed to stir for 3 h and monitored by TLC. After completion of the reaction, the product was extracted with chloroform and water, evaporated and column purification. (Eluent: 1:9 ethylacetate/n-hexane).

(*E*)-1,3,5-trimethyl-4-(phenyldiazenyl)-1*H*-pyrazole **(1e)**:

Orange solid, mp = 60-63 ºC, 189 mg, 88% yield. ^{1}H NMR (400MHz, $CDCl_3$) δ 2.50 (s, 3H), 2.57 (s, 3H), 3.77 (s, 3H), 7.35-7.38 (t, *J* = 7.0 Hz, 1H), 7.44-7.48 (t, *J* = 7.9 Hz, 2H), 7.77-7.79 (d, *J* = 8.1 Hz, 2H); ^{13}C NMR (100 MHz, $CDCl_3$) δ 10.1, 14.0, 36.1, 121.9, 129.0, 129.4, 135.2, 138.9, 142.5, 153.7; HRMS (ESI-TOF): calcd for $C_{12}H_{14}N_4$ $[M+H]^+$: 215.1297, found: 215.1291; IR (ATR, cm^{-1}): 1556, 1513, 1408, 766.

(E)-4-((3-fluorophenyl)diazenyl)-1,3,5-trimethyl-1H-pyrazole **(3e)**:

Yellow solid, mp = 45-48 ºC, 191 mg, 82% yield. ^{1}H NMR (400MHz, $CDCl_3$) δ 2.48 (s, 3H), 2.56 (s, 3H), 3.77 (s, 3H), 7.03-7.07 (t, *J* = 7.2 Hz, 1H), 7.38-7.47 (m, 2H), 7.58-7.60 (d, *J* = 7.9 Hz, 1H); ^{13}C NMR (100 MHz, $CDCl_3$) δ 10.0, 14.0, 36.1, 106.9 (d, *J* = 22.5 Hz), 116.0 (d, *J* = 22.0 Hz), 119.5 (d, *J* = 2.7 Hz), 130.1 (d, *J* = 8.6 Hz), 135.1, 139.6, 142.6, 155.3 (d, *J* = 6.8 Hz), 155.3 (d, *J* = 6.8 Hz), 163.4 (d, *J* = 244.9 Hz) ; HRMS (ESI-TOF): calcd for $C_{12}H_{13}FN_4$ $[M+H]^+$: 233.1202, found: 233.1191; IR (ATR, cm^{-1}): 1556, 1514, 1406, 1112, 784.

(*E*)-4-((3-chlorophenyl)diazenyl)-1,3,5-trimethyl-1*H*-pyrazole **(6e)**:

Yellow solid, mp = 90-93 ºC, 225 mg, 90% yield. ^{1}H NMR (400MHz, $CDCl_3$) δ 2.48 (s, 3H), 2.57 (s, 3H), 3.78 (s, 3H), 7.31-7.40 (m, 2H), 7.66-7.68 (d, *J* = 7.8 Hz, 1H), 7.75 (br, 1H); ^{13}C NMR (100 MHz, $CDCl_3$) δ 10.1, 14.1, 36.2, 120.8, 121.4, 129.1, 130.0, 135.0., 135.2, 139.7, 142.6, 154.6; HRMS (ESI-TOF): calcd for $C_{12}H_{13}ClN_4$ $[M+H]^+$: 249.0907, found: 249.0897; IR (ATR, cm^{-1}): 1556, 1514, 1403, 693, 784

(*E*)-4-((3-bromophenyl)diazenyl)-1,3,5-trimethyl-1*H*-pyrazole **(9e)**:

Yellow solid, mp = 99-102 ºC, 275 mg, 94% yield. ^{1}H NMR (400MHz, $CDCl_3$) δ 2.48 (s, 3H), 2.58 (s, 3H), 3.79 (s, 3H), 7.31-7.35 (t, *J* = 7.9 Hz, 1H), 7.47-7.49 (d, *J* = 7.6 Hz, 1H), 7.71-7.73 (d, *J* = 7.8 Hz, 1H), 7.90 (s, 1H); ^{13}C NMR (100 MHz, $CDCl_3$) δ 10.1, 14.1, 36.2, 121.9, 123.1, 123.8, 130.4, 132.0, 135.2, 139.7, 142.7, 154.7; HRMS (ESI-TOF): calcd for $C_{12}H_{13}BrN_4$ $[M+H]^+$: 293.0402, 295.0381 found: 293.0392, 295.0371; IR (ATR, cm^{-1}): 1514, 1555. 1401, 783, 703.

(*E*)-1,3,5-trimethyl-4-((3-(trifluoromethyl)phenyl)diazenyl)-1*H*-pyrazole **(15e)**:

Yellow solid, mp = 100-103 ºC, 255 mg, 90% yield. ^{1}H NMR (400MHz, $CDCl_3$) δ 2.51 (s, 3H), 2.61 (s, 3H), 3.81 (s, 3H), 7.56-7.64 (m, 2H), 7.95-7.97 (d, *J* = 7.6 Hz, 1H), 8.03 (s, 1H); ^{13}C NMR (100 MHz, $CDCl_3$) δ 10.1, 14.1, 36.1, 118.7 (q, *J* = 3.8 Hz), 122.8, 125.1, 125.6 (q, *J* = 2.4 Hz), 129.5, 131.5 (q, *J* = 32.3 Hz), 135.3, 139.8, 142.7, 153.7; HRMS (ESI-TOF): calcd for $C_{13}H_{13}F_3N_4$ $[M+H]^+$: 283.1171, found: 283.1163; IR (ATR, cm^{-1}): 1554, 1433, 1323, 1111, 801.

(*E*)-4-((3-methoxyphenyl)diazenyl)-1,3,5-trimethyl-1*H*-pyrazole **(18e)**:

Yellow solid, mp = 70-74 ºC, 275 mg, 85% yield. ^{1}H NMR (400MHz, $CDCl_3$) δ 2.50 (s, 3H), 2.57 (s, 3H), 3.78 (s, 3H), 3.88 (s, 3H), 6.93-6.95 (d, *J* = 6.9 Hz, 1H), 7.33-7.42 (m, 3H); ^{13}C NMR (100 MHz, $CDCl_3$) δ 10.1, 14.0, 36.1, 55.5, 105.6, 115.66, 115.69, 129.7, 135.2, 139.0, 142.6, 155.0, 160.3; HRMS (ESI-TOF): calcd for $C_{13}H_{16}N_4O[M+H]^+$: 245.1402, found: 245.1390; IR (ATR, cm^{-1}): 1556, 1514, 1407, 1130, 785.

Acknowledgements:

We are grateful to Science and Engineering Research Board (SERB), New Delhi for the financial support (EMR/2014/000780). The NMR, HRMS and other instrumentation facilities of IISER Mohali are greatly acknowledged. We are also thankful to IISER Mohali for the start-up grant and providing research facilities including computational facilities. SD thanks UGC for Junior and Senior Research Fellowships and MS thanks CSIR for Junior and Senior Research Fellowship. SG thanks IISER Mohali for the research fellowship. We extend our sincere thanks to Dr. Sabyasachi Rakshit and his group for helping in the UV-Vis kinetics measurements.

†Equally contribution

■ ASSOCIATED CONTENT

Supporting Information

The Supporting Information is available free of charge on the ACS Publications website at DOI:

UV-Vis photoswitching studies and kinetics data

NMR data of (***E***)- and (***Z***)- isomers of substituted phenylazopyrazole

Z-E Reverse isomerization kinetics plots of phenylazopyrazole derivatives

Computational data

Concentration dependency in NMR kinetics and association constant of **(*E*)-1d**

Photoswitching and kinetics data of **1d** in different solvents using UV-Vis spectroscopy

Hammett plots based on the UV-Vis spectroscopic kinetics data

Solvent effects in the *Z-E* isomerization rate of **1d**

^{1}H and ^{13}C-NMR spectral characterization data of arylazoacetylacetone derivatives **28c**, **31c**, **32c** and **38c**

^{1}H and ^{13}C-NMR spectral characterization data of arylazopyrazole derivatives (**1d-38d**)

^{1}H and ^{13}C-NMR spectral characterization data of *N*-methyl arylazopyrazole derivatives (**1e**, **3e**, **6e**, **9e**, **15e** and **18e**)

Cartesian coordinates of the optimized structures

(PDF)

■ AUTHOR INFORMATION

Corresponding Author

*E-mail: sugumarv@iisermohali.ac.in.

ORCID

Sugumar Venkataramani: 0000-0002-6465-3655

Mayank Saraswat: 0000-0003-1614-0262

Notes

The authors declare no competing financial interest.

References and Notes:

1. For example: (a) Koumura, N.; Zijlstra, R. W. J.; van Delden, R. A.; Harada, N.; Feringa, B. L. *Nature* **1999**, *401*, 152–155. (b) Eelkema, R.; Pollard, M. M.; Vicario, J.; Katsonis, N.; Ramon, Bastiaansen, C. W. M.; Broer, D. J.; Feringa, B. L. *Nature* **2006**, *440*, 163. (c) Feringa, B. L. *Acc. Chem. Res.* **2001**, *34*, 504–513. (d) Haberhauer, G.; Burkhart, C.; Woitschetzki, S.; Woelper, C. *J. Org. Chem.* **2015**, *80*, 1887–1895. (e) Hashim, P. K.; Thomas, R.; Tamaoki, N. *Chem. Eur. J.* **2011**, *17*, 7304 –7312.
2. For example: (a) Irie, M. *Chem. Rev.* **2000**, *100*, 1685−1716. (b) Sauer, M. *Proc. Natl. Acad. Sci. USA* **2005**, *102*, 9433–9434. (c) Garcia–Amoros, J.; Velasco, D. *Beilstein J. Org. Chem.* **2012**, *8*, 1003–1017. (d) Li, Z.; Wang, M.; Li, H.; He, J.; Li, N.; Xu, Q.; Lu, J. *J. Mater. Chem. C* **2017,** *5*, 8593–8598. (e) Zhang, J.; Zou, Q.; Tian, H. *Adv. Mater.* **2013**, *25*, 378–399. (f) Dong, H.; Zhu, H.; Meng, Q.; Gong, X.; Hu, W. *Chem. Soc. Rev.* **2012**, *41*, 1754–1808.

3. For example: (a) Hunter, C. A.; Togrul, M.; Tomas, S. *Chem. Commun.* **2004**, 108–109. (b) Goodman, A.; Breinlinger, E.; Ober, M.; Rotello, V. M. *J. Am. Chem. Soc*. **2001**, *123*, 6213–6214. (c) Nalluri, S. K. M.; Ravoo, B. J. *Angew. Chem., Int. Ed*. **2010**, *49*, 5371–5374. (d) Yamaguchi, H.; Kobayashi, Y.; Kobayashi, R.; Takashima, Y.; Hashidzume, A.; Harada, A. *Nat. Commun.* **2012**, *3*, 1617/1–1617/5. (e) Gao, Z.; Han, Y.; Chen, S.; Li, Z.; Tong, H.; Wang, F. *ACS Macro Lett.* **2017**, *6*, 541–545. (f) Chen, J.; Serizawa, T.; Komiyama, K. *Angew. Chem., Int. Ed*. **2009**, *48*, 2917–2920.
4. For example: (a) Chambers, J. J.; Kramer, R. H. *Methods Cell Biol.* **2008**, *90*, 217–232. (b) Banghart, M.; Borges, K.; Isacoff, E.; Trauner, D.; Kramer, R. H. *Nat. Neurosci*. **2004**, *7*, 1381–1386. (c) Sun, Y.; Ma, J.; Zhang, F.; Zhu, F.; Mei, Y.; Liu, L.; Tian, D.; Li, H. *Nature Commun*. **2017**, *8*, 1–5. (d) Liu, T.; Bao, C.; Wang, H.; Lin, Y.; Jia, H.; Zhu, L. *Chem. Commun.* **2013**, *49*, 10311–10313. (e) Ying, Y. L.; Zhang, J.; Meng, F. N.; Cao, C.; Yao, X.; Willner, I.; Tian, H.; Long, Y. T. *Sci. Rep.* **2013**, *3*:1662, 1–8.
5. For example: (a) Zhang, X.; Hou, L.; Samori, P. *Nature Commun.* **2016**, *7*, 11118. (b) Do, K.; Boxer, S. G. *J. Am. Chem. Soc.* **2013**, *135*, 10226−10229. (c) Wencel, D.; Abel, T.; McDonagh, C. *Anal. Chem.* **2014**, *86*, 15−29.
6. For example: (a) Stoll, R. S.; Hecht, S. *Angew. Chem., Int. Ed.* **2010**, *49*, 5054–5075. (b) Peter, M. V.; Stoll, R. S.; Kuehn, A.; Hecht, S. *Angew. Chem., Int. Ed.* **2008**, *47*, 5968–5972. (c) Blanco, V.; Leigh, D. A.; Marcos, V. *Chem. Soc. Rev.* **2015**, *44*, 5341–5370. (d) Viehmann, P.; Hecht, S. *Beilstein J. Org. Chem.* **2012**, *8*, 1825–1830. (e) Neri, S.; Martin, S. G.; Pezzato, C.; Prins, L. J. *J. Am. Chem. Soc.* **2017**, *139*, 1794−1797.
7. Dugave, C.; Demange, L. *Chem. Rev.* **2003**, *103*, 2475−2532. (and references within)
8. Merino, E.; Ribagorda, M. *Beilstein J. Org. Chem.* **2012**, *8*, 1071–1090.
9. For example: (a) Xia, X.; Yu, H.; Wang, L.; ul–Abdin, Z. *RSC Adv.* **2016**, *6*, 105296–105316. (b) Kulikovska, O.; Goldenberg, L. M.; Stumpe, J. *Chem. Mater.* **2007**, *19*, 3343–3348. (c) Ge, J.; Yin, Y. *Angew. Chem., Int. Ed.* **2011**, *50*, 1492–1522. (d) Guo, S.; Matsukawa, K.; Miyata, T.; Okubo, T.; Kuroda, K.; Shimojima, A. *J. Am. Chem. Soc.* **2015**, *137*, 15434–15440. (e) Kobatake, S.; Takami, S.; Muto, H.; Ishikawa, T.; Irie, M. *Nature*, **2007**, *446*, 778 –781.
10. For example: (a) Izquierdo–Serra, M.; Gascon–Moya, M.; Hirtz, J. J.; Pittolo, S.; Poskanzer, K. E.; Ferrer, E.; Alibes, R.; Busque, F.; Yuste, R.; Hernando, J.; Gorostiza, P. *J. Am. Chem. Soc.* **2014**, *136*, 8693–8701. (b) Mahimwalla, Z.; Yager, K. G.; Mamiya, J.; Shishido, A.; Priimagi, A.; Barrett, C. J. *Polym. Bull.* **2012**, *69*, 967–1006. (c) Beharry, A. A.; Woolley, G. A. *Chem. Soc. Rev.* **2011**, *40*, 4422–4437. (d) Fujita, D.; Murai, M.; Nishioka, T.; Miyoshi, H. *Biochemistry* **2006**, *45*, 6581–6586. (e) Mart, R. J.; Allemann, R. K. *Chem. Commun.* **2016**, *52*, 12262–12277.
11. For example: (a) Lerch, M. M.; Hansen, M. J.; van Dam, G. M.; Szymanski, W.; Feringa, B. L. *Angew. Chem., Int. Ed.* **2016**, *55*, 10978–10999. (b) Sheldon, J. E.; Dcona, M. M.; Lyons, C. E.; Hackett, J. C.; Hartman, M. C. T. *Org. Biomol. Chem.* **2016**, *14*, 40–49. (c) Velema, W. A.; Hansen, M. J.; Lerch, M. M.; Driessen, A. J. M.; Szymanski, W.; Feringa, B. L. *Bioconjugate Chem.* **2015**, *26*, 2592–2597. (d) Broichhagen, J., Frank, J. A., Johnston, N. R,

Mitchell, R. K., Smid, K., Marchetti, P., Bugliani, M., Rutter, G. A, Trauner, D., Hodson, D. J. *Chem Comm*. **2015**, *51*, 6018–6021. (e) Velema, W. A.; van der Berg, J. P.; Hansen, M. J.; Szymanski, W.; Driessen, A. J. M.; Feringa, B. L. *Nat. Chem.* **2013**, *5*, 924–928.

12. For example: (a) Rau, H.; Lueddecke, E. *J. Am. Chem. Soc.* **1982**, *104*, 1616–1620. (b) Crecca, C. R.; Roitberg, A. E. *J. Phys. Chem. A* **2006**, *110*, 8188–8203. (c) Hoffman, D. P.; Ellis, S. R.; Mathies, R. A. *J. Phys. Chem. A* **2013**, *117*, 11472–11478. (d) Stuart, C. M.; Frontiera, R. R.; Mathies, R. A. *J. Phys. Chem. A* **2007**, *111*, 12072–12080. (e) Fujino, T.; Tahara, T. *J. Phys. Chem. A* **2000**, *104*, 4203–4210. (f) Quick, M.; Dobryakov, A. L.; Gerecke, M.; Richter, C.; Berndt, F.; Ioffe, I. N.; Granovsky, A. A.; Mahrwald, R.; Ernsting, N. P.; Kovalenko, S. A. *J. Phys. Chem. B* **2014**, *118*, 8756–8771. (g) Lednev, I. K.; Ye, T. Q.; Hester, R. E.; Moore, J. N., *J. Phys. Chem.* **1996**, *100*, 13338–13341. (h) Cui, G.; Guan, P. J.; Fang, W. H. *J. Phys. Chem. A* **2014**, *118*, 4732–4739.
13. For example: (a) Nerbonne, J. M.; Weiss, R. G. *J. Am. Chem. Soc.* **1978**, *100*, 5953–5954. (b) Titov, E.; Lysyakova, L.; Lomadze, N.; Kabashin, A. V.; Saalfrank, P.; Santer, S. *J. Phys. Chem. C* **2015**, *119*, 17369–17377. (c) Ikegami, T.; Kurita, N.; Sekino, H.; Ishikawa, Y. *J. Phys. Chem. A* **2003**, *107*, 4555–4562. (d) Joshi, N. K.; Fuyuki, M.; Wada, A. *J. Phys. Chem. B* **2014**, *118*, 1891–1899. (e) Cembran, A.; Bernardi, F.; Garavelli, M.; Gagliardi, L.; Orlandi, G. *J. Am. Chem. Soc.* **2004**, *126*, 3234–3243. (f) Simeth, N. A.; Crespi, S.; Fagnoni, M.; König, B. *J. Am. Chem. Soc.* **2018**, *140*, 2940–2946.
14. Bandara, H. M. D.; Burdette, S. C. *Chem. Soc. Rev.* **2012**, *41*, 1809–1825.
15. For example: (a) Bleger, D.; Schwarz, J.; Brouwer, A. M.; Hecht, S. *J. Am. Chem. Soc.* **2012**, *134*, 20597–20600. (b) Beharry, A.; Sadovski, O.; Woolley, G. A. *J. Am. Chem. Soc.* **2011**, *133*, 19684–19687. (c) Samanta, S.; McCormick, T. M.; Schmidt, S. K.; Seferos, D. S.; Woolley, G. A. *Chem. Commun.* **2013**, *49*, 10314–10316. (d) Bleger, D.; Hecht, S. *Angew. Chem., Int. Ed.* **2015**, *54*, 11338–11349.
16. For example: (a) Huang, Y. G.; Shiota, Y.; Su, S. Q.; Wu, S. Q.; Yao, Z. S.; Li, G. L.; Kanegawa, S.; Kang, S.; Kamachi, T.; Yoshizawa, K.; Ariga, K.; Sato, O. *Angew. Chem., Int. Ed.* **2016**, *55*, 14628–14632. (b) Venkataramani, S.; Jana, U.; Dommaschk, M.; Soennichsen, F. D.; Tuczek, F.; Herges, R. *Science* **2011**, *331*, 445–448. (c) Dommaschk, M.; Peters, M.; Gutzeit, F.; Schuett, C.; Naether, C.; Soennichsen, F. D.; Tiwari, S.; Riedel, C.; Boretius, S.; Herges, R. *J. Am. Chem. Soc.* **2015**, *137*, 7552–7555. (d) Wang, Y.; Ge, X.; Schull, G.; Berndt, R.; Tang, H.; Bornholdt, C.; Koehler, F.; Herges, R. *J. Am. Chem. Soc.* **2010**, *132*, 1196–1197. (e) Iranpoor, N.; Firouzabadi, H.; Khalili, D.; Motevalli, S. *J. Org. Chem.* **2008**, *73*, 4882–4887.
17. For example: (a) Byabartta, P. *Int. J. Curr. Res. Chem. Pharm. Sci.* **2015**, *2*, 75-81. (b) Pandey, P.; Maheshwari, N.; Dave, A. *J. Liq. Chromatogr.* **1991**, *14*, 3311–3315. (c) Jain, R.; Agarwal, D. D.; Goyal, R. N.; Fresenius, Z. *Anal. Chem.* **1979**, *298*, 44. (d) Pradhan, S.; Mondal, S.; Sinha, C. *J. Indian Chem. Soc.* **2015**, *93*, 1067–1084. (e) Al-Saleh, B.; El-Apasery, M. A.; Elnagdi, M. H. *J. Chem. Res.* **2004**, 578–580. (f) Al-Shiekh, M. A.; Salah El-Din, A. M.; Hafez, E. A.; Elnagdi, M. H. *J. Heterocycl. Chem.* **2004**, *41*, 647–654. (g) Khound, S.; Das, P. J. *Indian J. Chem., Sect. B* **1998**, *37B*, 155–157.

18. Wendler, T.; Schuett, C.; Naether, C.; Herges, R. *J. Org. Chem.* **2012**, *77*, 3284–3287.
19. Weston, C. E., Richardson, R. D., Haycock, P. R., White, A. J. P., Fuchter, M. J. *J. Am. Chem. Soc*. **2014**, *136*, 11878−11881.
20. For example: (a) Weston, C. E.; Kramer, A.; Colin, F.; Yildiz, O.; Baud, M. G. J.; Meyer–Almes, F.J.; Fuchter, M. J. *ACS Infect. Dis*. **2017**, *3*, 152–161. (b) Stricker, L.; Fritz, E. C.; Peterlechner, M.; Doltsinis, N. L.; Ravoo, B. J. *J. Am. Chem. Soc.* **2016**, *138*, 4547–4554. (c) Ghebreyessus, K.; Cooper, S. M. Jr. *Organometallics* **2017**, *36*, 3360–3370.
21. Calbo, J.; Weston, C. E.; White, A. J. P.; Rzepa, H.; Contreras–García, J.; Fuchter, M. J. *J. Am. Chem. Soc.* **2017**, *139*, 1261–1274.
22. (a) Sharma, P.; Kumar, A.; Upadhyay, S.; Singh, J.; Sahu, V. *Med. Chem. Res.* **2010**, *19*, 589−602. (b) Marten, J.; Seichter, W.; Weber, E. *Z. Anorg. Allg. Chem.* **2005**, *631*, 869−877. (c) Burra, V. R.; Reddy, N. B.; Ravidranath, L. K. *Pharma Chem.* **2015**, *7*, 43−48. (d) Han, X.; Zhu, X.; Hong, Z.; Wei, L.; Ren, Y.; Wan, F.; Zhu, S.; Peng, H.; Guo, L.; Rao, L.; Feng, L.; Wan, J. *J. Chem. Inf. Model.* **2017**, *57*, 1426−1438. (e) Kunitomo, J.; Yoshikawa, M.; Fushimi, M.; Kawada, A.; Quinn, J. F.; Oki, H.; Kokubo, H.; Kondo, M.; Nakashima, K.; Kamiguchi, N.; Suzuki, K.; Kimura, H.; Taniguchi, T. *J. Med. Chem.* **2014**, *57*, 9627−9643. (f) Kale, P. D. *J. Chem. Pharm. Res.* **2013**, *5*, 130−134.
23. The fraction of *Z*- and *E*-isomers present in the mixture at PSS from UV spectroscopic data has been estimated using the literature procedures (ref. 19 and Cho, E. N.; Zhitomirsky, D.; Han, G. G. D.; Liu, Y.; Grossman, J. C. *ACS Appl. Mater. Interfaces* **2017**, *9*, 8679−8687.) Using the composition, and the absorption maxima corresponding to the π–π* and n–π* transitions of the Z-isomer, their respective molar extinction coefficients have been estimated with an uncertainty 2-5% (as indicated by Fuchter and coworkers in reference 19).
24. Based on the kinetics experiments using UV-Vis spectroscopy and Taft plot (Figure 4), it is evident that the aryl substitutions at the *ortho* position destabilize the *Z*-isomers due to steric reasons. At NMR concentrations both steric factors as well as hydrogen bonding were operative that further increases the rate of thermal reverse isomerizations. Considering this fact, and also for understanding the dominant influence among electronic effects and the hydrogen bonding, NMR kinetics studies have been primarily focussed on *meta*- and *para*-substituted arylazopyrazole derivatives. The results of the kinetics studies are discussed in the section D and E.
25. For the thermal reverse *Z-E* isomerization, we have also considered the rotation mechanism. However, the transition state corresponding to the rotation about the N=N group could not be located. Indeed, the inversion pathway has been reported to be the lower energy pathway (as mentioned in the ref. 21). Through potential energy surface scan calculations, we found out that the rotation channel has almost twice in energy relative to the inversion channel for **1d**. (See Figure S4 in SI).
26. As phenylazopyrazole derivatives are unsymmetrical azoarenes, the two possible transition states corresponding to the inversion at azo nitrogens connected either to phenyl or to pyrazole rings have been computed. Using the estimated barriers, the weighted average half-lives and rate constants have been estimated based on the population differences between the two transition states. (as mentioned in the ref. 21)

27. (a) Taft, R. W. *J. Am. Chem. Soc.* **1952**, *74*, 2729−2732. (b) Fujita, T.; Takayama, C.; Nakajima, M. *J. Org. Chem.* **1973**, *38*, 1623-1630.
28. Hammett, L. P. *J. Am. Chem. Soc.* **1937**, *59*, 96-103.
29. Nishimura, N.; Sueyoshi, T.; Yamanaka, H.; Imai, E.; Yamamoto, S.; Hasegawa, S. *Bull. Chem. Soc. Jpn.* **1976**, *49*, 1381−1387.
30. (a) Thordarson, P. *Chem. Soc. Rev.* **2011**, *40*, 1305−1323. (b) Hibbert, D. B.; Thordarson, P. *Chem. Commun.* **2016**, *52*, 12792−12805. (c) The non-linear fitting has been performed using the web based bindfit program available as open access in the website: www.supramolecular.org
31. (a) Lubbe, A. S.; Kistemaker, J. C. M.; Smits, E. J.; Feringa, B. L. *Phys. Chem. Chem. Phys.* **2016**, *18*, 26725−26735. (b) Gille, K.; Knoll, H.; Quitzsch, K. *Int. J. Chem. Kinet.* **1998**, *31*, 337−350. (c) Serra, F.; Terentjev, E. M. *Macromolecules* **2008**, *41*, 981−986.
32. *Solvents and Solvent Effects in Organic Chemistry*; Reichardt, C.; Welton, T., 4th Ed.; Wiley-VCH: Weinheim, 2011.
33. Kamlet, M. J.; Abboud, J. L. M.; Abraham, M. H.; Taft, R. W. *J. Org. Chem.* **1983**, *48*, 2877−2887.
34. Marcus, Y. *Chem. Soc. Rev.* **1993**, *22*, 409−416.
35. Cerón-Carrasco, J. P.; Jacquemin, D.; Laurence, C.; Planchat, A.; Reichardt, C.; Sraïdi, K. *J. Phys. Org. Chem.* **2014**, *27*, 512–518.
36. Otsuki, J.; Suwa, K.; Sarker, K. K.; Sinha, C. *J. Phys. Chem. A* **2007**, *111*, 1403−1409.
37. Stratmann, R. E.; Burant, J. C.; Scuseria, G. E.; Frisch, M. J. *J. Chem. Phys.* **1997**, *106*, 10175−10183.
38. Becke, A. D. *J. Chem. Phys.* **1993**, *98*, 5648−5652.
39. Zhao, Y.; Truhlar, D. G. *Theor. Chem. Acc.* **2008**, *120*, 215−241.
40. Francl, M. M.; Pietro, W. J.; Hehre, W. J.; Binkley, J. S.; Gordon, M. S.; Defrees, D. J.; Pople, J. A. *J. Chem. Phys.* **1982** , *77*, 3654−3665.
41. Miertuš, S.; Scrocco, E.; Tomasi, J. *Chem. Phys.* **1981**, 55, 117−129.
42. Halgren, T. A.; Lipscomb, W. N. *Chem. Phys. Lett.* **1977**, *49*, 225−232.
43. Fukui, K. *Acc. Chem. Res.* **1981**, *14*, 363−368.
44. (a) Carpenter, J. E.; Weinhold, F. *J. Mol. Struct.: THEOCHEM* **1988**, *169*, 41−62. (b) Foster, J. P.; Weinhold, F. *J. Am. Chem. Soc.* **1980**, *102*, 7211−7218.
45. Wiberg, K. B. *Tetrahedron* **1968**, *24*, 1083−1096.
46. Gaussian 09, revision D.01: Frisch, M. J.; Trucks, G. W.; Schlegel, H. B.; Scuseria, G. E.; Robb, M. A.; Cheeseman, J. R.; Scalmani, G.; Barone, V.; Mennucci, B.; Petersson, G. A.; Nakatsuji, H.; Caricato, M.; Li, X.; Hratchian, H. P.; Izmaylov, A. F.; Bloino, J.; Zheng, G.; Sonnenberg, J. L.; Hada, M.; Ehara, M.; Toyota, K.; Fukuda, R.; Hasegawa, J.; Ishida, M.; Nakajima, T.; Honda, Y.; Kitao, O.; Nakai, H.; Vreven, T.; Montgomery, J. A., Jr.; Peralta, J. E.; Ogliaro, F.; Bearpark, M.; Heyd, J. J.; Brothers, E.; Kudin, K. N.; Staroverov, V. N.; Keith, T.; Kobayashi, R.; Normand, J.; Raghavachari, K.; Rendell, A.; Burant, J. C.; Iyengar, S. S.; Tomasi, J.; Cossi, M.; Rega, N.; Millam, J. M.; Klene, M.; Knox, J. E.; Cross, J. B.; Bakken, V.; Adamo, C.; Jaramillo, J.; Gomperts, R.; Stratmann, R. E.; Yazyev, O.; Austin, A. J.; Cammi, R.; Pomelli, C.; Ochterski, J. W.; Martin, R. L.; Morokuma, K.; Zakrzewski, V. G.; Voth, G. A.; Salvador, P.; Dannenberg, J. J.; Dapprich, S.;

Daniels, A. D.; Farkas, O.; Foresman, J. B.; Ortiz, J. V.; Cioslowski, J.; Fox, D. J. Gaussian, Inc., Wallingford, CT, 2013.

47. (a) Diau, E. W. -G. *J. Phys. Chem. A* **2004**, *108*, 950−956. (b) Crecca, C. R.; Roitberg, A. E. *J. Phys. Chem. A* **2006**, *110*, 8188−8203.

TOC